

Document downloaded from:

<http://hdl.handle.net/10251/102250>

This paper must be cited as:



The final publication is available at

<http://doi.org/10.1016/J.ECOINF.2017.10.008>

Copyright Elsevier

Additional Information

1 **Revisiting probabilistic neural networks: a comparative study**
2 **with support vector machines and the microhabitat suitability**
3 **for the Eastern Iberian chub (*Squalius valentinus*)**

4

5 Rafael Muñoz-Mas^{1*}, Shinji Fukuda², Javier Pórtoles³, Francisco Martínez-Capel¹

6 ¹ Institut d'Investigació per a la Gestió Integrada de Zones Costaneres (IGIC),

7 Universitat Politècnica de València, C/ Paranimf 1 – Grau de Gandia 46730, País Valencià,
8 (Spain).

9 ² Institute of Agriculture, Tokyo University of Agriculture and Technology, Saiwai-cho 3-5-8,
10 Fuchu, Tokyo 183-8509, (Japan).

11 ³ Fundación para la Investigación del Clima, C/ Tremps 11, Madrid 28040, (Spain).

12

13 *Correspondence to: Rafael Muñoz-Mas, e-mail: rafa.m.mas@gmail.com, voice: +34
14 622098521

15

16 **Keywords**

17 differential evolution

18 habitat suitability model

19 Iberian Peninsula

20 machine learning

21 partial dependence plot

22 species distribution model

23

24 **Abstract**

25 Probabilistic Neural Networks (PNNs) and Support Vector Machines (SVMs) are flexible
26 classification techniques suited to render trustworthy species distribution and habitat
27 suitability models. Although several alternatives to improve PNNs' reliability and
28 performance and/or to reduce computational costs exist, PNNs are currently not well
29 recognised as SVMs because the SVMs were compared with standard PNNs. To rule out this
30 idea, the microhabitat suitability for the Eastern Iberian chub (*Squalius valentinus* Doadrio &
31 Carmona, 2006) was modelled with SVMs and four types of PNNs (homoscedastic,
32 heteroscedastic, cluster and enhanced PNNs); all of them optimised with differential
33 evolution. The fitness function and several performance criteria (correctly classified
34 instances, true skill statistic, specificity and sensitivity) and partial dependence plots were
35 used to assess respectively the performance and reliability of each habitat suitability model.
36 Heteroscedastic and enhanced PNNs achieved the highest performance in every index but
37 specificity. However, these two PNNs rendered ecologically unreliable partial dependence
38 plots. Conversely, homoscedastic and cluster PNNs rendered ecologically reliable partial
39 dependence plots. Thus, Eastern Iberian chub proved to be a eurytopic species, presenting
40 the highest suitability in microhabitats with cover present, low flow velocity (approx. 0.3
41 m/s), intermediate depth (approx. 0.6 m) and fine gravel (64–256 mm). PNNs outperformed
42 SVMs; thus, based on the results of the cluster PNN, which also showed high values of the
43 performance criteria, we would advocate a combination of approaches (e.g., cluster &

44 heteroscedastic or cluster & enhanced PNNs) to balance the trade-off between accuracy
45 and reliability of habitat suitability models.

46

47 **1 Introduction**

48 Humans have facilitated species extinctions, invasions, increased soil erosion, altered fire
49 frequency and hydrology, and incited profound changes in primary productivity and other
50 key biogeochemical and ecosystems processes (Ellis et al., 2010). Therefore, in the face of
51 this global change, forecasting future ecosystem states, such as future species geographic
52 distributions or land-use patterns, is currently a central priority in biogeographical and
53 ecological sciences (Eberenz et al., 2016; Evans et al., 2016). As a consequence of this
54 priority, scientists, conservationists and managers are repeatedly compelled to confront
55 new problems requiring data analysis (LaDeau et al., 2016).

56 Data analysis is largely classified into two broad categories: unsupervised and supervised
57 (Olden et al., 2008). The former focus on revealing patterns and structures in data (e.g.,
58 finding groups of co-occurring species), such as the renowned Self-Organising Maps (SOM)
59 (Kohonen, 1982) or the laureate t-Distributed Stochastic Neighbour Embedding (t-SNE) (Van
60 Der Maaten and Hinton, 2008). Conversely, supervised approaches, such as decision trees
61 (e.g., CART; Breiman et al., 1984) or the Generalised Additive Models (GAMs) (Hastie and
62 Tibshirani, 1990), attempt to model the relationship between a set of inputs and known
63 outputs (Olden et al., 2008). Based on the nature of the outputs, supervised learning is
64 likewise classified into two main groups. Therefore, if the outputs are continuous, the

65 supervised technique is used to perform regression (e.g., M5; Quinlan, 1992), whereas for
66 categorical outputs the task is termed classification, although intermediate approaches exist
67 (i.e., ordinal regression) (Gutierrez et al., 2016).

68 Currently, a number of different approaches to perform classification are available: from
69 the simple k -nearest algorithm, which assigns an object to the most common class among a
70 k number of neighbours; to the complex deep neural networks that have won numerous
71 contests in pattern recognition thanks to their structure, which consists of a vast number of
72 interconnected neurons disposed in multiple layers (Schmidhuber, 2015). Recent
73 applications in ecology and species distribution modelling of both extremes of this range
74 can be found within scientific literature (e.g., Abdollahnejad et al., 2017; Chen et al., 2014).

75 However, the most popular approaches (e.g., GAMs) are those of intermediate complexity
76 located in the middle of this broad spectrum of alternatives (e.g., Muñoz-Mas et al., 2016d).

77 A multitude of different model categories coexist under the umbrella-term classification,
78 therefore, classification techniques such as GAMs are considered to be a purely statistic
79 approach, while others, such as artificial neural networks (e.g., Multi-Layer Perceptrons –
80 MLPs) (Werbos, 1982; McCulloch and Pitts, 1943), are included within the machine learning
81 and computer science discipline (Olden et al., 2008).

82 Currently, machine learning algorithms, which make vast use of techniques from
83 mathematical programming and statistics (Sousa et al., 2013), are routinely used to address
84 classification tasks in almost every area of knowledge (Oliva and Cuevas, 2017). Among
85 them, one prominent classification activity is the development of species distribution
86 models, or habitat suitability models, to explore species ecology and predict their

87 occurrence under different management and climatic scenarios (Bennetsen et al., 2016;
88 Guisan et al., 2013). However, habitat suitability modelling has several characteristics that
89 are not present in other environmental classification tasks that may determine the
90 performance and reliability of the models (Elith and Graham, 2009). Species rarity (Wisz et
91 al., 2008), which usually conditions the number of independent observations of the target
92 organism and the close-related data prevalence (i.e., the proportion of presences in a data
93 set) (Fukuda and De Baets, 2016; Mouton et al., 2009), may eventually compromise the
94 performance of the models. Moreover, the susceptibility of the modelling technique to
95 regularisation (i.e., adequate control of parameter tuning and easy selection of variables to
96 prevent overfitting) (Reineking and Schröder, 2006) can affect the credibility of the
97 classifier. Nonetheless, each modelling technique has its own unique characteristics; thus,
98 despite recent advances in Artificial Intelligence (AI), an optimal technique that can be
99 indiscriminately applied can never be envisaged (Yano, 2016; Crisci et al., 2012).

100 Since the industrial revolution, worldwide human impacts on landscapes and river systems
101 have intensified significantly (Habersack et al., 2014). Therefore, one area of research that
102 has grown steadily in the last few decades is that of ecohydraulics (Casas-Mulet et al.,
103 2016). Ecohydraulics is principally addressed to study the relationship between hydraulics
104 (e.g., water depth or flow velocity) and biota to perform environmental flow assessments.
105 In accordance, an enormous number of different techniques have been used to develop the
106 necessary habitat suitability models for riparian and aquatic organisms, from fuzzy logic
107 (Mouton et al., 2009; Rüger et al., 2005) to random forests (Vezza et al., 2015; Fukuda et al.,
108 2014). Nevertheless, the aforementioned GAMs and MLPs (R Muñoz-Mas et al., 2016b;

109 Jowett and Davey, 2007) are well represented, while papers employing multiple techniques
110 can no longer be considered a rarity (R Muñoz-Mas et al., 2016a; Fukuda et al., 2013).
111 Although environmental flow assessment should focus on the different components of
112 riparian ecosystems (Poff et al., 2010), it has traditionally focused on fish species (Tharme,
113 2003) because they occupy relatively high trophic levels and a broad set of habitats must
114 typically be present to complete their life cycle (R Muñoz-Mas et al., 2016c). Consequently,
115 they have been considered adequate indicators of in-stream habitat constraints (Lorenz et
116 al., 2013). Furthermore, although freshwater fish can be considered a well-studied group,
117 new species continue to be described (Tierno de Figueroa et al., 2013). Therefore, 79 new
118 species of freshwater fishes, such as the Eastern Iberian chub (*Squalius valentinus* Doadrio
119 & Carmona, 2006), have been described in the Mediterranean basin since 2000 (Tierno de
120 Figueroa et al., 2013). In this region, with a high number of endemisms, 70% of the
121 freshwater fish species are either threatened with extinction or already extinct, which is the
122 highest proportion anywhere in the world (Maceda-Veiga, 2013). Native fish have suffered
123 from multiple and recurrent introductions, particularly since 1850, which has been
124 highlighted as one of the main negative factors affecting their survival (R Muñoz-Mas et al.,
125 2016d; Tricarico, 2012). In accordance, within the Mediterranean basin, new habitat
126 suitability models are continuously being developed, both for the invasive and the
127 threatened native species e.g., (e.g., Muñoz-Mas et al., 2016e, 2017; Boavida et al., 2014).
128 A relatively unknown classification technique within ecological literature in general, and
129 ecohydraulics in particular, are Probabilistic Neural Networks (PNNs) (Specht, 1989, 1990).

130 PNNs are machine learning classifiers that combine the Bayes theorem for decision-making,
131 which assigns an object to the class that presents the highest value in the corresponding
132 true posterior Probability Density Function (PDF) (e.g., $\text{PDF}_{\text{class i}} > \text{PDF}_{\text{class j}}$), with the Parzen-
133 Rosenblatt window method (Parzen, 1962; Rosenblatt, 1956) to estimate the empirical PDF
134 from a finite data sample (Jin et al., 2002). Although PNNs have been traditionally
135 considered to be a kind of artificial neural network (Bishop, 1995), they differ substantially
136 from other artificial neural networks, such as MLPs; thus, optimising PNNs requires the
137 optimisation of very few parameters (typically only one). This parameter can be set
138 manually (Muñoz-Mas et al., 2014). Therefore, the PNN has been considered to be a one-
139 pass learning approach (Specht, 1990).

140 PNNs have been proven to be proficient in various tasks, such as: risk assessment (Adeli and
141 Panakkat, 2009), bacterial growth prediction (Hajmeer and Basheer, 2002), fault detection
142 (Chang et al., 2009) or cancer diagnosis (Berrar et al., 2003). Conversely, to the best of our
143 knowledge, there are very few examples of their use in ecology, despite their having
144 demonstrated great performance (Muñoz-Mas et al., 2014; Siira et al., 2009; Corne et al.,
145 2004) and stability over various prevalence datasets (Muñoz-Mas et al., 2014). Nonetheless,
146 the latter is an advantage over other approaches that require case weighting (Platts et al.,
147 2008) or resampling (Allouche et al., 2006). In addition, PNNs have displayed great flexibility
148 in encompassing the hydraulic niche (i.e., discriminating the suitable microhabitats)
149 compared to other approaches that have been considered to be excessively rigid (Muñoz-
150 Mas et al., 2014).

151 Another machine learning approach that showed great flexibility in general (Belousov et al.,
152 2002), and in particular with determining suitable microhabitats (R Muñoz-Mas et al.,
153 2016a), is that of Support Vector Machines (SVMs) (Vapnik, 1995). Habitat suitability
154 models developed with SVMs proved very accurate when compared with other machine
155 learning classification approaches (R Muñoz-Mas et al., 2016d; Fukuda et al., 2013). As with
156 PNNs, SVMs only require the optimisation of very few parameters (Fukuda and De Baets,
157 2016; Huang and Wang, 2006). Previous comparisons between PNNs and SVMs typically
158 judged SVMs as the preferable option (e.g., Modaresi and Araghinejad, 2014; Muniz et al.,
159 2010; Öğüt et al., 2009). However, since their inception, PNNs have been the subject of
160 scientific research to improve their performance (Ahmadlou and Adeli, 2010) and/or reduce
161 the computational burden (Kusy and Zajdel, 2015; Miguez et al., 2010; Li and Ma, 2008;
162 Berthold and Diamond, 1998). Consequently, the conclusions of these comparisons may
163 have varied if any of the aforementioned methods to improve PNNs had been employed.
164 In order to scrutinise the real capabilities of PNNs, we compared four different approaches
165 to develop PNNs with standard SVMs and demonstrated that SVMs do not mandatorily
166 outperform PNNs. The paper is structured as follows: section 2 describes the fundamentals
167 of PNNs and the four different approaches followed to develop PNNs, the theory and
168 settings of SVMs, the optimisation approach for PNNs and SVMs, the training dataset and
169 the comparison performed. In section 3, the accuracy of the four different approaches and
170 the SVM and the reliability of the modelled habitat suitability are presented. In section 4,
171 the results are discussed and integrated with current literature. Finally, the conclusions are
172 provided in section 5.

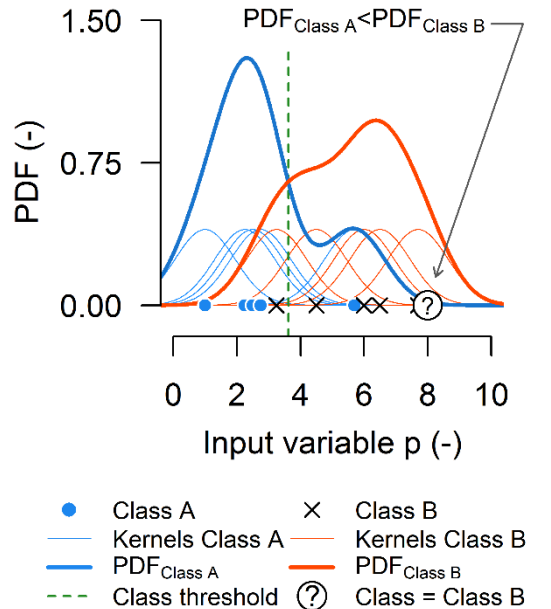
173

174 **2 Methods**

175 **2.1 Probabilistic Neural Networks – PNNs**

176 Following the precepts of the Bayes theorem, PNNs classify a given input pattern (i.e., a
177 string encompassing one record of each of the p input variables) to the class that presents
178 the highest value among the posterior PDFs (Zhong et al., 2007). However, these PDFs are
179 typically unknown (Hajmeer and Basheer, 2002); thus, PNNs circumvent this limitation by
180 employing the Parzen-Rosenblatt window method (Parzen, 1962; Rosenblatt, 1956), or
181 kernel density estimation, to calculate empirical PDFs based on the training patterns (i.e.,
182 the strings encompassing, each one, one record of each of the p input variables) included in
183 the training dataset (Jin et al., 2002). The main idea behind the Parzen-Rosenblatt method is
184 approximating the PDF by a sum of continuous distribution functions or kernels centred at
185 each training pattern (Adeli and Panakkat, 2009), which have smoothing parameters (σ_j)
186 that control the degree of influence (i.e., the window) of each training pattern towards each
187 coordinate (Fig. 1).

188



189

190 Fig. 1. Example of the classification of an unknown input pattern (?) based on the Bayes theorem
 191 and the Parzen-Rosenblatt method to calculate the Probability Density Function (PDF) as the sum of
 192 Gaussian kernel functions centred at the training patterns.

193

194 Although the kernel function can be chosen from a number of alternatives (e.g., uniform,
 195 triangular or Epanechnikov), the bell-shaped normal Gaussian kernel is the most common
 196 choice (Kusy and Zajdel, 2015; Modaresi and Araghinejad, 2014; Jin et al., 2002). In
 197 accordance, the formula used to calculate the multivariate PDF that combines all the input
 198 patterns and variables for each class m is:

199

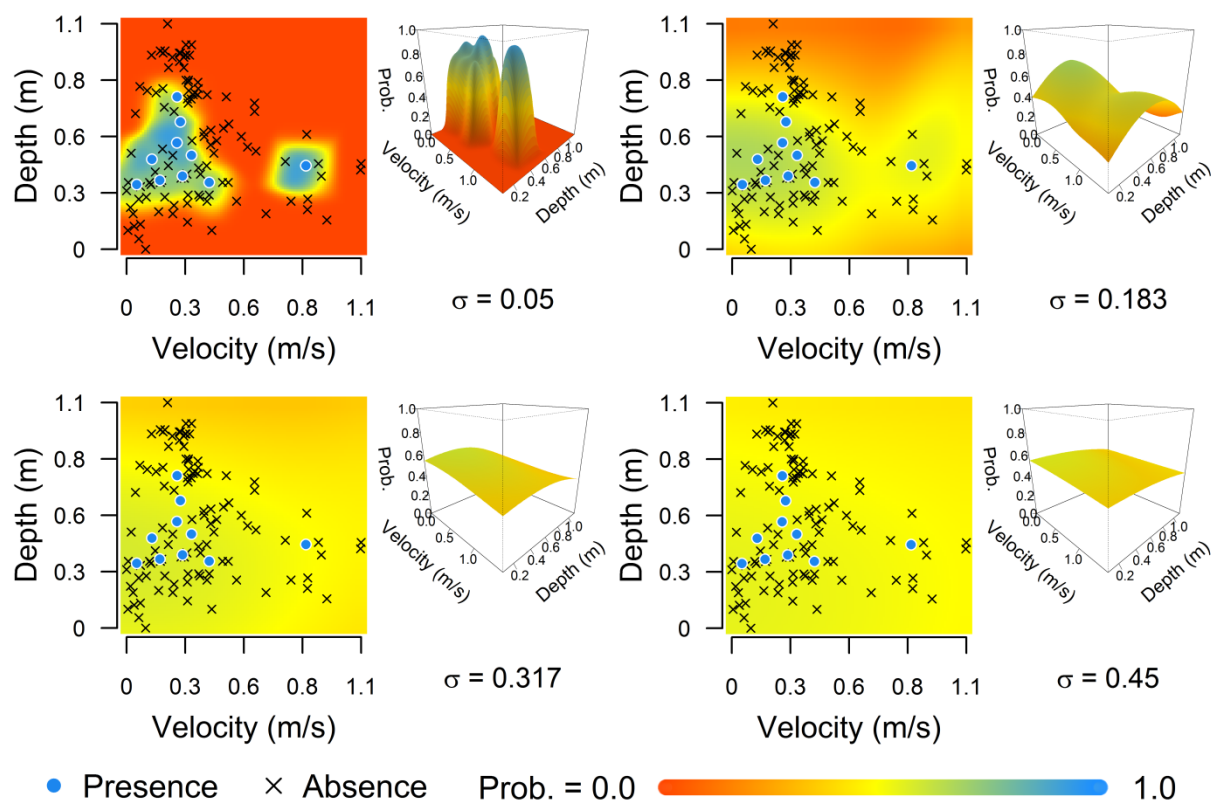
200
$$PDF_{class\ m}(x) = \frac{1}{(2\pi)^{p/2} \prod_{j=1}^p \sigma_j^n} \sum_{i=1}^n \exp \left[-\sum_{j=1}^p \frac{(x_j - X_j^i)^2}{2\sigma_j^2} \right]; \text{ (Equation 1)}$$

201

202 where x is the input pattern to be classified and x_j its j^{th} element (corresponding to the p
 203 input variables included in the training dataset), and X^n is the i^{th} training pattern belonging
 204 to the class for which the PDF is being calculated, whereas X_j^i corresponds to its j^{th} element

205 (also corresponding to the p input variables) with n equal to the number of training
 206 patterns for class m (i.e., the total number of training patterns for the class m). The σ_j are
 207 the window or smoothing parameters, which determine the window of the kernel around
 208 the mean of the p input variables. Therefore, small values of σ_j produce spiked PDFs with
 209 the maxima narrowly centred at the training patterns, whereas large values of σ_j produce
 210 smooth PDFs with the maxima instead centred at the region that gathers the maximum
 211 number of training patterns (i.e., the region of maximum density of several training
 212 patterns) (Fig. 2).

213

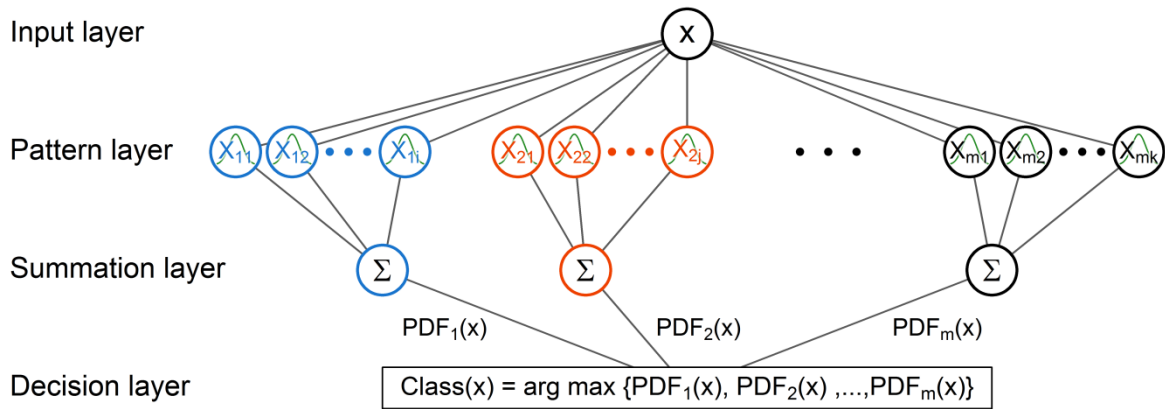


214

215 Fig. 2. Effect of the kernel window or smoothing parameter σ on the probability of presence, in a
 216 presence-absence classification task, rendered by an homoscedastic Probabilistic Neural Network
 217 (PNN) where the smoothing parameter is equalled for each input variables or coordinate (i.e.,
 218 $\sigma_{Velocity} = \sigma_{Depth}$).
 219

220 The novelty of the method proposed by Specht (1990, 1989) consisted of breaking up the
221 entire process into a large number of simple processes implemented in a four-layered feed-
222 forward network topology that first calculates the PDFs, following the Parzen-Rosenblatt
223 approach, and then assigns the input pattern to the corresponding class (i.e., solves the
224 inequality of the Bayes theorem) (Fig. 3) (Berrar et al., 2003). The input layer is merely used
225 to supply the input patterns to the pattern layer. The pattern layer has as many nodes as
226 available training patterns and computes the value of each Gaussian kernel function at the
227 input pattern (i.e., at the evaluated point) accounting for the selected smoothing
228 parameters. The summation layer computes the value of the PDF at the input pattern for
229 each class m . It is carried out by adding up the outputs of the preceding pattern layer and
230 taking into account the class of the pattern neurons. Consequently, each neuron of this
231 layer is exclusively connected to the pattern neurons corresponding to the same class while
232 the final value is divided by the number of patterns of the corresponding class (n) impeding
233 the immediate assignment of the assessed pattern to the outnumbering class (i.e., PNNs are
234 insensitive to data prevalence) (Muñoz-Mas et al., 2014). This is an advantage of PNNs over
235 other machine learning approaches (Muñoz-Mas et al., 2014). Finally, the decision layer
236 compares the values of the PDFs and employs the arguments of the maxima (arg max) to
237 assign the input pattern to the class that presents the highest value among the PDFs. The
238 values of the PDFs are previously standardised by dividing them by the sum of the values of
239 each PDF; thus, the probabilistic outputs are rendered (adding up to one) in addition to the
240 winning class.

241



242
243
244
245
246

Fig. 3. General architecture of a Probabilistic Neural Network (PNN) where a given input pattern x is classified within a set of m classes. The multi-stemmed architecture is reduced to the two coloured branches depicted on the left when two class problems (e.g., presence-absence) are addressed.

247 2.1.1 Homoscedastic PNN

248 This approach is by far the most common way to develop PNN models (e.g., Modaresi and
249 Araghinejad, 2014; Muniz et al., 2010; Öğüt et al., 2009) because it corresponds to the very
250 basic implementation of PNN (Specht, 1989, 1990). The smoothing parameter is equalled
251 for each input variables (i.e., $\sigma_1 = \sigma_2 = \dots = \sigma_p$); thus, the influence of each pattern on
252 each coordinate coincides (Fig. 4 – Upper left panel). In accordance, a single scalar σ
253 requiring optimisation is used for all pattern neurons (Kusy and Zajdel, 2015). The tested
254 values of the smoothing parameter σ ranged between zero and one (Table 1) (Muñoz-Mas
255 et al., 2014; Muniz et al., 2010).

256

257 2.1.2 Heteroscedastic PNN

258 Although homoscedastic PNNs demonstrated great performance, a single global smoothing
259 parameter σ may be insufficient to achieve the desired accuracy (Chang et al., 2009). By
260 adapting separate smoothing parameters for each coordinate or variable (i.e., $\sigma_1 \neq \sigma_2 \neq$

261 $\dots \neq \sigma_p$), the classification accuracy can be greatly improved (Specht and Romsdahl, 1994),
262 as has been corroborated by a number of studies (e.g., Kusy and Zajdel, 2015; Li and Ma,
263 2008). This type of model is a more elastic classifier, since, in such a case, the influence of
264 each variable on neighbouring points differs (Fig. 4 – Upper right panel) (Kusy and Zajdel,
265 2015). Thus, the number of smoothing parameters requiring optimisation equalled the
266 number of input variables, and the tested ranges for these parameters (σ_j) also ranged
267 between zero and one (Table 1) (Muñoz-Mas et al., 2014; Verma, 2008).

268

269 **2.1.3 Cluster PNN**

270 One of the major disadvantage of PNN stems from the fact that it requires one node or
271 neuron for each training pattern, which increases the computational burden (Specht, 1992).
272 Therefore, promptly after their inception, researchers offered various improvements to
273 reduce the number of pattern neurons and hence the computational costs (e.g., Berthold
274 and Diamond, 1998; Burrascano, 1991; Yang and Chen, 1998). Among these improvements,
275 those based on data clustering stood out (Specht, 1992). Nonetheless, depending on the
276 clustering approach, they can be very efficient compared to other approaches that may be
277 inefficient because they need several iterations to converge (e.g., Berthold and Diamond,
278 1998). Consequently, these approaches rely in a sequential use of unsupervised (clustering)
279 and supervised (PNNs) techniques; thus, cluster PNNs can be homoscedastic,
280 heteroscedastic or enhanced.

281 Currently, a number of different clustering algorithms have been used as pre-treatments
282 prior to the development of cluster PNNs, such as global k-means (Chang et al., 2009) or j-

means (Li and Ma, 2008) (Fig. 4 – Lower left panel). However, over the last 50 years, thousands of clustering algorithms have been published; thus, a number of alternatives are available (Jain, 2010). We advocated the *k*-medoids algorithm (Kaufman and Rousseeuw, 1987) as implemented within the *R* package *cluster* (Maechler et al., 2016). This algorithm clusters data around *k* representative objects or prototypes, named medoids, by minimising the distance between the input patterns and them; thus, it represents a more robust version of *k*-means (Maechler et al., 2016). In addition, they proved to be fast and the actual implementation within the *cluster* package allows one single cluster to be rendered. Therefore, with regard to the example problem of presence-absence, the selection of one single presence pattern and a number of absence patterns surrounding it will fit well the theory around the use of convex hulls (Cornwell et al., 2006) to determine the n-dimensional hypervolume to describe the ecological niche (sensu Hutchinson, 1957). To better illustrate the capabilities of clustering as a pre-treatment, the optimal number of clusters for each class was sought simultaneously with one single smoothing parameter (i.e., homoscedastic PNNs). Therefore, three parameters required optimisation. The maximum number of clusters allowed equalled the maximum number of patterns of the class with the smallest sample size, which for the presence-absence example problem coincided with the sample size of the presence class whereas the single σ ranged between zero and one (Table 1) (Muñoz-Mas et al., 2014; Muniz et al., 2010). The number (#) of clusters was obtained by rounding up the real values (\mathbb{R}) given by the optimisation algorithm. Therefore, for the specific example, the # clusters were $Class_{presence} = \|\vec{v_1}\|$ and #

304 clusters $Class_{absence} = \|\vec{v}_2\|$ where \vec{v} is the optimal solution, which encodes the best
305 parameters in a vector or chromosome (see below).

306

307 2.1.4 Enhanced PNN

308 In both the aforementioned approaches (homoscedastic and heteroscedastic PNNs) the
309 selected smoothing parameter is used as a global parameter without considering any
310 probable local densities or heterogeneity in the training data (Ahmadlou and Adeli, 2010).

To overcome this limitation, a method to improve standard PNNs – named enhanced PNNs – was proposed (Ahmadlou and Adeli, 2010). Enhanced PNNs incorporate local information and existing inhomogeneity, modifying the smoothing parameter of each training pattern in accordance with the proportion of data for the corresponding class within a predefined hypersphere (local circle) of radius r (i.e., calculating the proportion of cases of each class and for each pattern below a Euclidean distance r) (Fig. 4 – Lower right panel). As a consequence, the smoothing parameter for each training pattern varies as follows:

318

$$\sigma_{mi} = \alpha_{mi} \times \sigma; \text{ (Equation 2)}$$

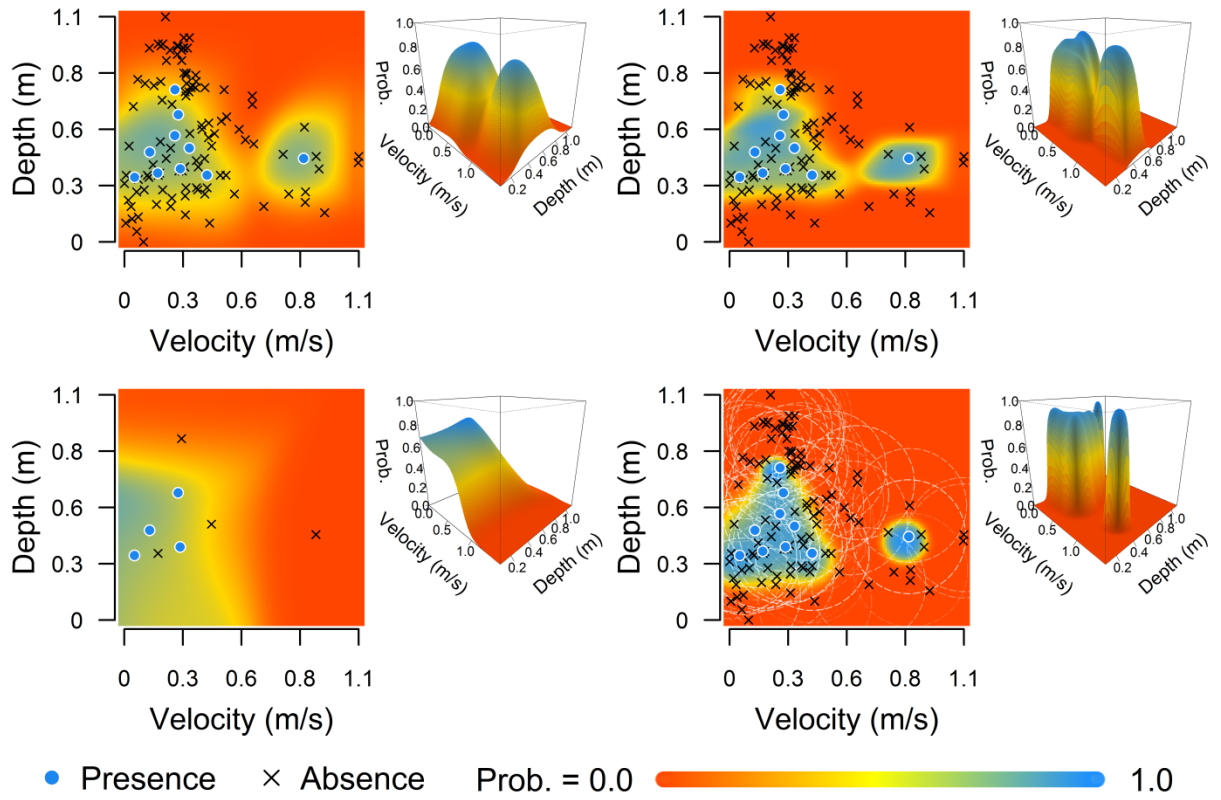
320

321 where, σ corresponds to the base smoothing parameter, α_{mi} the proportion of training
 322 patterns within the local circle for the training pattern i that belongs to the class m . Finally,
 323 σ_{mi} corresponds to the resulting smoothing parameter. In this regard, enhanced PNNs can
 324 be viewed as an extension of the heteroscedastic PNNs, where each training pattern
 325 presents its own smoothing parameter (Kusy and Zajdel, 2015). However, only two different

326 parameters (σ and r), require optimisation. The smoothing parameter σ ranged between
327 zero and one and the radius of local circles r between zero and two, which for the example
328 problem, with four rescaled variables, coincided with the maximum possible distance
329 between two training patterns (Table 1) (Ahmadlou and Adeli, 2010). The *R* code to
330 implement the four approaches, which is based on the *R* package *pnn* (Chasset, 2013), can
331 be found in Appendix A.

332 Table 1. Range of the tested parameter settings for the four alternative methods to develop Probabilistic Neural Networks (PNNs) (smoothing
 333 parameters σ_j , number of cluster centres and radius of the local circles r) and the Support Vector Machine (SVM) (radial basis kernel function
 334 width γ and regularisation parameter C) for the example presence-absence problem.

	Homoscedastic PNN	Heteroscedastic PNN	Cluster PNN	Enhanced PNN	SVM
σ_j	Min.	0	0	0	0
	Max.	1	1	1	1
# clusters	Min.			1	
	Max.		Min{N _{class pres.} , N _{class abs.} }		
r	Min.			0	
	Max.			Max. Euclidean dist.	
γ	Min.			0	
	Max.			1	
C	Min.			0	
	Max.			500	



335

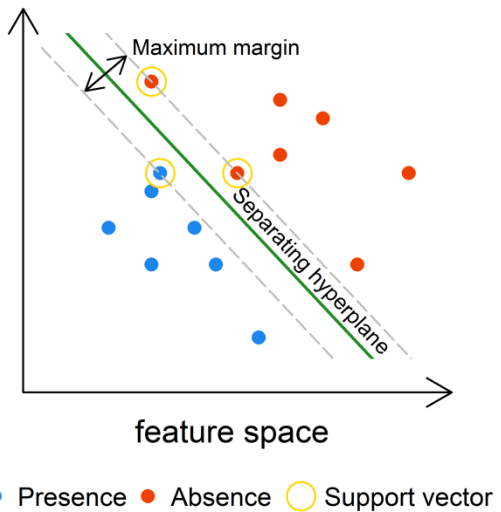
336 Fig. 4. Example of the differences in the final probability of presence, in a presence-absence
 337 classification task, obtained with the four alternative types of Probabilistic Neural Networks (PNNs).
 338 The example is based on a random data sample. The upper left panel corresponds to a
 339 homoscedastic PNN with one single smoothing parameter (σ), the upper right panel to a
 340 heteroscedastic PNN with one smoothing parameter per input variable ($\sigma_{Velocity}$ & σ_{Depth}), the
 341 lower left panel to a cluster PNN with four clusters per class and one single smoothing parameter
 342 (σ) and the lower right panel to an enhanced PNN with local decision circles ($\alpha_i \times \sigma$).
 343

344 2.2 Support Vector Machines – SVMs

345 Support Vector Machines (SVMs) is a machine learning approach that employs discriminant
 346 hyperplanes to classify the input data (Vapnik, 1995). The fundamental of SVMs, addressed
 347 to two-class problems, is to construct an Optimal Separating Hyperplane (OSH), which
 348 corresponds to one of the infinite number of existing separating hyperplanes that lie
 349 furthermore from both classes, and hence maximises the margin. The margins of the OSH
 350 are determined by some cases (i.e., training patterns) which are the so-called support

351 vectors (Fig. 5) (Moguerza and Muñoz, 2006). If the discriminant function between classes is
352 not linear, then the data is projected into a higher-dimensional space (i.e., the feature
353 space) where these data can be linearly separated. This projection is carried out by
354 employing a class of functions called kernels, which perform a nonlinear transformation of
355 the original data. Among these kernel functions, the most popular are polynomial, radial
356 basis and sigmoid (R Muñoz-Mas et al., 2016d; Howley and Madden, 2005). However, in
357 practice, Gaussian Radial Basis Functions (RBFs) have demonstrated to be sufficient to
358 accurately model many real problems (Wu et al., 2012), including habitat suitability
359 modelling (R Muñoz-Mas et al., 2016a; Fukuda et al., 2013). The RBFs exclusively require the
360 optimisation of the kernel width (i.e., the γ parameter), which is related to the variance of
361 the data, and thus determines the radius of influence of samples selected by the model as
362 support vectors. If the problem remains not linearly separable after the kernel
363 transformation, then the misclassified observations can be penalised by a regularisation
364 parameter (C), which defines the trade-off between margin maximisation and error
365 minimisation.

366



367

368 Fig. 5. Optimal Separating Hyperplane (OSH) and selected support vectors in a presence-absence
369 toy example.

370

371 The SVMs were developed in *R* (R Core Team, 2015) with the function *svm* implemented
372 within the package *e1071* (Dimitriadou et al., 2011). The selected mapping function was the
373 RBF; thus, the parameters C and γ required optimisation. The tested ranges of the
374 parameters were based on Huang and Wang (2006) and ranged from 0 to 500 and 0 to 1 for
375 C and γ respectively (Table 1). Data prevalence affects the performance of SVMs; thus
376 unbalanced datasets may tip the balance towards the outnumbering class (Osuna et al.,
377 1997). In accordance, as with previous studies (R Muñoz-Mas et al., 2016d), each class was
378 weighted by the complementary of its class prevalence (i.e., $1 - prevalence_{class\ m}$).
379 Therefore, the weights used in the example presence-absence problem were 0.06 for the
380 absence class and 0.94 for the presence class (see below for a detailed description of the
381 training dataset).

382

383 **2.3 Parameter optimisation with Differential Evolution (DE)**

384 Although the parameter requiring optimisation could have been set by employing grid
385 searches (Öğüt et al., 2009), the use of population-based algorithms (e.g., evolutionary and
386 genetic algorithms or particle swarm optimisation) is the most popular approach (Narimani
387 and Narimani, 2013; Miguez et al., 2010; Jin et al., 2002). Therefore, in order to decrease
388 computational cost, a metaheuristic population-based algorithm – the Differential Evolution
389 (DE) algorithm (Storn and Price, 1997) – was used to optimise: the smoothing parameters,
390 the best number of clusters for each class, the radius of the local decision circles and the C
391 and γ parameters of the SVM. The DE algorithm is an evolutionary algorithm inspired by
392 Darwin's process of natural selection and particularly suited to optimise real-valued
393 functions of real-valued parameters (Ardia et al., 2011; Mullen et al., 2011). A user defined
394 number of potential solutions (population) are encoded in vectors (chromosomes or agents)
395 of real-values, and the associated performance (fitness) is calculated for each of these
396 potential solutions (Ardia et al., 2011). Each generation consists of evolving (i.e., creating) a
397 new population from the former population members by mutating and crossing the former
398 population through arithmetic operations, such as addition and subtraction, whose
399 frequency and intensity depends on the parameter settings (Mullen et al., 2011). At each
400 generation, once the entire population has been evolved, only those child vectors that
401 present better fitness substitute their parents (Ardia et al., 2011). The algorithm stops after
402 a specified number of generations, or after the objective function value associated with the
403 best member has been reduced below a specified value (Mullen et al., 2011).

404 The DE implementation used was that of the *R* package *DEoptim* (Ardia et al., 2011; Mullen
405 et al., 2011) and the optimisation took place following a repeated *k*-fold scheme.
406 Specifically, it followed a three times threefold cross-validation scheme ($3 \times$
407 $3_{cross-validation}$) because it proved to be adequate to induce genetically optimised habitat
408 suitability models (Rafael Muñoz-Mas et al., 2016; Stein et al., 2005). In addition, every fold
409 presented similar prevalence to the original dataset (i.e., similar proportion of training
410 patterns for each class). The models were optimised based on a fitness function (equation
411 3) encompassing several indices arising from the confusion matrix (Table 2) and especially
412 addressed to stimulate over-prediction (Specificity \leq Sensitivity) (R Muñoz-Mas et al.,
413 2016d, 2016b) because it has been affirmed to be more reliable – from an ecological
414 viewpoint – than under-prediction (Mouton et al., 2010):

415

416
$$Fitness = \frac{1}{3 \times 3} \sum_{i=1}^{3 \times 3} TSS_i + \min\{0, Sn_i - Sp_i\}; \text{ (Equation 3)}$$

417

418 where *Sn* (*Sensitivity*) corresponds to the ratio of presences correctly classified (i.e., $Sn =$
419 $\frac{TP}{TP+FN}$), *Sp* (*Specificity*) corresponds to the ratio of absences correctly classified (i.e., $Sp =$
420 $\frac{TN}{FP+TN}$) and *TSS* (*True Skill Statistic*) to the sum of sensitivity and specificity minus one (i.e.,
421 $TSS = Sn + Sp - 1$) (Mouton et al., 2010). In addition, these indices and Correctly
422 Classified Instances or *CCI* (i.e., $CCI = \frac{TP+TN}{TP+FP+TN+FN}$) were used to evaluate the
423 performance of the different models.

424

425 Table 2. Confusion matrix for a two-class problem (e.g., presence-absence). The acronyms
426 correspond to: True Positive (TP), False Positive (FP), False Negative (FN) and True Negative (TN).

		Observed	
		Presence	Absence
Predicted	Presence	TP	FP
	Absence	FN	TN

427

428 The entire process was fully parallelised employing the 7 cores of an Intel® Core™ i7-
429 4702MQ 2.20GHz with 8GB of RAM while the parameter settings of the optimisation were
430 based on the recommendations described in Mullen et al. (2011) and the package vignette
431 (Table 3), although these parameter settings may also require optimisation to address
432 problems of higher complexity (see e.g., Gibbs et al., 2008). Once the best parameters had
433 been determined, a single model for each alternative approach to develop PNNs and the
434 SVM was trained to perform the subsequent analyses (R Muñoz-Mas et al., 2016d; Fukuda
435 et al., 2013).

436

437 Table 3. Differential Evolution (DEOptim) parameter settings. Default values were used in the
 438 unlisted arguments.

Operator	Argument name	DEoptim (DE) Setting	Function
Value to be reached	VTR	1	The optimisation stops when this value is achieved.
Evolving strategy	strategy	2	Method employed for mutating and crossing the former population; strategy = 2 corresponds to a uniform mutation operator.
Population size	NP	$10 \times \# \text{ parameters}$	Number of population members.
Maximum iterations allowed	itermax	$10 \times \# \text{ parameters}$	Maximum number of generations.
Crossover adaptation	c	0.7	Parameter controlling the crossover. Higher values upweight child vectors.
Relative convergence tolerance	reltol	0.0005	The algorithm stops after <i>steptol</i> generations if the absolute improvement of the fitness is lower than <i>reltol</i> .
Step tolerance	steptol	$5 \times \# \text{ parameters}$	See <i>reltol</i> .
Crossover probability	CR	0.5	Fraction of the parameter values that are copied from the mutant.

439

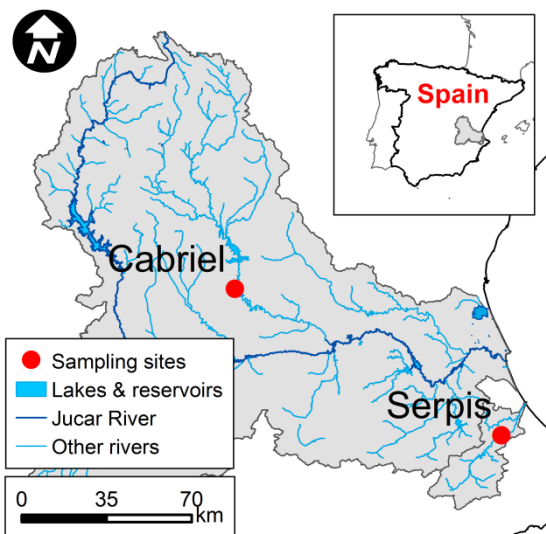
440 2.4 The training dataset

441 Although the use of virtual species or in silico datasets is gaining adepts (e.g., Fukuda and
 442 De Baets, 2016), we employed a real dataset encompassing the difficulties enumerated in
 443 the introduction. The occurrence data for the Eastern Iberian chub were collected at the
 444 microhabitat scale (i.e., few m² with homogeneous depth, velocity, substrate and cover)
 445 during summer low flows (2006) in two separated river stretches of two perennial rivers of
 446 the Jucar River Basin District (Fig. 6). The first was located in the Cabriel River (main Jucar
 447 River tributary), and the second in the Serpis River.

448 The Eastern Iberian chub is a small cyprinid (maximum body length = 17.5 cm) (Alcaraz-
 449 Hernández et al., 2015) that inhabits the Spanish Levantine region (Perea and Doadrio,
 450 2015). This vulnerable species, whose populations showed marked decreasing trends (IUCN,

451 2016), occurs principally in streams with clear waters and gravel bottom and prefers
452 moderate flowing stretches (Doadrio and Carmona, 2006).

453



454

455 Fig. 6. Location of the sampling sites for Eastern Iberian chub (*Squalius valentinus* Doadrio &
456 Carmona, 2006) within the Cabriel (main Jucar River tributary) and Serpis River basins.

457

458 In order to diminish the bias derived from an unbalanced sampling effort over habitat units

459 of fast-flow (e.g. rapid or riffle) and slow-flow (e.g. glide or pool) nature, we selected similar

460 areas (approximately 250 m²) of these two gross categories (Muñoz-Mas et al., 2012).

461 Following common procedures (see Muñoz-Mas et al., 2014, 2012), the microhabitat study

462 was conducted by underwater observation (snorkelling). The depth, velocity, substrate and

463 cover for the presence data were measured at fish locations, whereas the absence data

464 were collected following a systematic sampling approach (Bovee, 1986). Particularly, these

465 variables were measured in a uniform grid, of approximately 1.5 m² per cell, completely

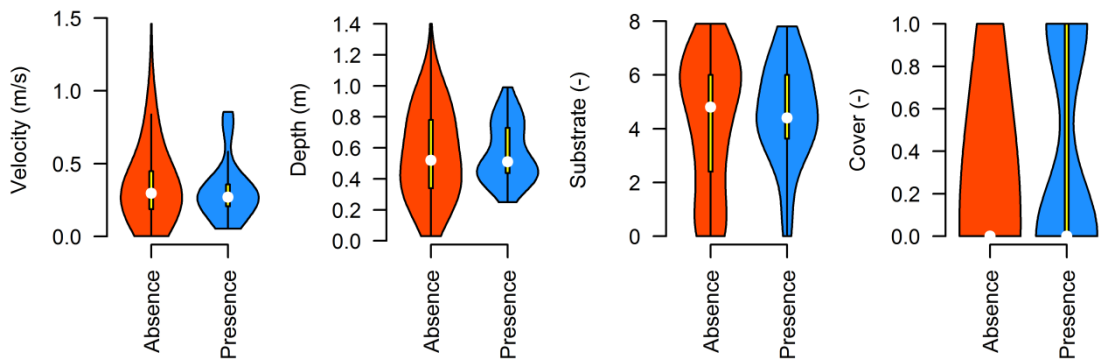
466 covering the sampled habitats. Velocity (m/s) was measured with an electromagnetic

467 current meter (Valeport®, United Kingdom) and depth (m) was measured with a wading rod

468 to the nearest cm. The percentage of each substrate class (i.e., bedrock, boulders, cobbles,
469 gravel, fine gravel, sand, silt and vegetated silt) was visually estimated following the
470 guidelines used in previous studies (e.g., Muñoz-Mas et al., 2012), and these percentages
471 were converted into the substrate index (-) (Mouton et al., 2011) that presents values from
472 zero (vegetated silt) to eight (bedrock). In addition, the presence-absence of cover in the
473 form of: aquatic vegetation, caves, log jams, shade or rocks, was also recorded. These types
474 of cover summarise the concept of structural cover (e.g., boulders, log jams) (Bovee et al.,
475 1998) and escape cover (e.g. vegetation, caves) (Raleigh et al., 1986) and, based on the
476 maximum body size of the species, they were considered present (i.e., one) when any of
477 them occupied an area larger than 0.5 × 0.5 m.

478 In the end, the Eastern Iberian chub was observed in 40 microhabitats (14 in the Cabriel
479 River and 26 in the Serpis River), whereas the absence data were collected at 607 different
480 microhabitats (304 in the Cabriel River and 303 in the Serpis River). Therefore, the training
481 dataset presented a prevalence of 0.06. The Eastern Iberian chub occurred more frequently
482 at intermediate velocity and depth, when compared with the absence data, it occurred at
483 finer substrates (substrate index = 4) (Fig. 7). Finally, the presence data collected at
484 microhabitats with cover outnumbered the data collected at those with no cover.
485 The input data involved different units and spanned different ranges, which may lead some
486 variables to dominate the classification (Li and Ma, 2008). Therefore, following previous
487 studies (e.g., Ben-Hur and Weston, 2010; Hajmeer and Basheer, 2002), the input dataset
488 was rescaled between zero and one. This rescaled dataset was used to train the different
489 PNNs and the SVM.

490



491

492 Fig. 7. Violin plots of the data on Eastern Iberian chub (*Squalius valentinus* Doadrio & Carmona,
493 2006) presence and absence collected in the Cabriel and Serpis Rivers.

494

495 2.5 Model evaluation

496 Developing ecologically reliable habitat suitability models requires balancing the accuracy
497 and complexity of the model via regularisation (Reineking and Schröder, 2006). Otherwise
498 the developed models may violate the ecological gradient theory, which states that species
499 responses to environmental variables are likely to be monotone or unimodal with different
500 degrees of skewness (Austin, 2007).

501 In order to scrutinise the modelled relationship between the input variables and the
502 probability of presence, partial dependence plots (Friedman, 2001) – based on the code
503 implemented within the package *randomForests* (Liaw and Wiener, 2002) – were developed
504 for each model. Partial dependence plots depict the average of the response variable (i.e.,
505 probability of presence) vs a gradient of the inspected predictor variable and accounting for
506 the effects of the remaining variables within the model by averaging their effects
507 (Friedman, 2001). The standard implementation, which consist of first substituting the
508 inspected variable with values along its range to then calculate the mean effect on the

509 response variable (i.e., probability of presence), has been demonstrated to be a useful tool
510 in a number of studies (e.g., Muñoz-Mas et al., 2016b; Shiroyama and Yoshimura, 2016;
511 Vezza et al., 2015). However, averaging the effects of the remaining variables may mask
512 variables interactions (Zurell et al., 2012; Evans et al., 2011). Therefore, instead of one
513 single line chart depicting the mean value vs the gradient of the inspected variable (Ω_z),
514 every 100-quantil or percentile ($Q_z(s)$) was depicted for every value in Ω_z to get a better
515 insight of the modelled habitat suitability. The partial dependence was computed for each
516 of 50 equally spaced values over the range of each examined variable ($m = 50$) except for
517 cover, which is a dichotomous variable ($m = 2$). Therefore, for each predictor (z) within the
518 original training dataset (X) several values along the inspected gradient were calculated
519 following Equation 4:

520

$$\Omega_z = \left\{ \min(X_z) + \left(\frac{\max(X_z) - \min(X_z)}{m-1} \times k \right) \mid k = 0, \dots, m-1 \right\}; \text{(Equation 4)}$$

522

523 where $\min(X_z)$ and $\max(X_z)$ correspond respectively to the minimum and maximum
524 entries of the inspected variable (X_z) included in X with $z \in \{1, \dots, p\}$ and p equalling the
525 number of predictor variables included in the training dataset (in the example problem $p =$
526 4). Then, for each value included in Ω_z a modified dataset ($X_z(s)$) is obtained, with $z \in$
527 $\{1, \dots, p\}$ and $s \in \Omega_z$, by substituting X_z in X by the corresponding value of Ω_z . Then, the
528 resulting dataset $X_z(s)$ is evaluated with the model for which the partial dependence plots
529 are being calculated (i.e., $g(\cdot)$ that can be one of the four different PNNs or the SVM) and

530 the percentiles of the cumulative distribution function $Q_z(s)$, as defined by Gumbel (1939),
531 are calculated ($F(\cdot)$) following Equation 5:

532

533
$$Q_z(s) = F(g(X_z(s))); \text{ (Equation 5)}$$

534

535 **3 Results**

536 **3.1 Performance**

537 The *DEOptim* algorithm rendered values for the smoothing parameters σ_j for three out of
538 four of the models in a relatively narrow range (i.e., σ from 0.091 to 0.364). Conversely, the
539 parameter for variable velocity in the heteroscedastic PNN presented the smallest ($\sigma_{\text{velocity}} =$
540 0.030) (Table 4). The latter value contributed to the ecologically unreliable partial
541 dependence plot for this variable (see below).

542

543 Table 4. Best parameters obtained for the four different approaches to develop Probabilistic Neural
544 Networks (PNNs) and the Support Vector Machine (SVM).

Model	Optimal parameters
Homoscedastic PNN	$\sigma = 0.106$
Heteroscedastic PNN	$\sigma_{\text{velocity}} = 0.030; \sigma_{\text{depth}} = 0.091; \sigma_{\text{substrate}} = 0.211; \sigma_{\text{cover}} = 0.187$
Cluster PNN	$\# \text{clusters}_{\text{presence}} = 22; \# \text{clusters}_{\text{absence}} = 20; \sigma = 0.136$
Enhanced PNN	$\sigma = 0.364; r = 0.196$
SVM	$C = 24.789; \gamma = 0.163$

545

546 Enhanced PNN and heteroscedastic PNN achieved the highest values of the fitness function,
547 although the enhanced PNN presented lower variability (Table 5). Regarding the
548 performance criteria used for model evaluation, Heteroscedastic and cluster PNNs

549 presented the best accuracy (CCI) but heteroscedastic PNN presented the highest True Skill
550 Statistic (TSS). Finally, enhanced PNN rendered the best Sensitivity (Sn) whereas the best
551 Specificity (Sp) was obtained with cluster PNN. Looking at the probability of presence
552 rendered in addition to the winning class, the four methods to develop PNN rendered
553 outputs covering the entire feasible output range (i.e., from zero to one) whereas the
554 maximum value obtained with SVM, which alters the classification threshold, was only 0.1
555 (see also Fig. 9).

556 The optimisation of the SVM took the shortest time and the heteroscedastic PNN the
557 longest, which was in line with the number of pattern neurons of the PNN and the searching
558 effort, which rose in accordance with the number of optimised parameters (Table 5). The
559 SVM presented the smallest ratio between the number of parameters optimised vs time,
560 whereas among the four approaches to develop PNN, the homoscedastic PNN (tight
561 followed by cluster PNN) presented the smallest ratio and the heteroscedastic PNN the
562 highest.

563

564

565 Table 5. Model performance and confidence interval to evaluate the four different approaches to
 566 develop Probabilistic Neural Networks (PNNs) and the Support Vector Machine (SVM): Fitness (Eq.
 567 3), Correctly Classified Instances (CCI), True Skill Statistics (TSS), Sensitivity (Sn), Specificity (Sp) and
 568 minimum (Min.) and maximum (Max.) values of the probability of presence obtained during the $3 \times$
 569 3 cross-validation (nine models) and the lapse of the optimisation (Optimisation was parallelised in
 570 an Intel core i7). The best results are in bold.

		Cross-validation					Time (min)	
	Fitness	CCI	TSS	Sn	Sp	Min.	Max.	
Homoscedastic PNN	0.34±0.17	0.65±0.05	0.39±0.10	0.75±0.13	0.64±0.06	0.0	1.0	6.10
Heteroscedastic PNN	0.45±0.12	0.68±0.04	0.47±0.07	0.80±0.09	0.67±0.05	0.0	1.0	73.04
Cluster PNN	0.39±0.14	0.68±0.04	0.44±0.08	0.76±0.11	0.68±0.05	0.0	1.0	22.52
Enhanced PNN	0.45±0.09	0.65±0.04	0.46±0.08	0.82±0.09	0.64±0.05	0.0	1.0	32.60
SVM	0.33±0.15	0.67±0.04	0.38±0.07	0.71±0.1	0.67±0.05	0.0	0.1	3.85

571

572 3.2 Partial dependence plots

573 The four tested approaches (Fig. 8) and the SVM (Fig. 9) modelled similar habitat suitability
 574 (i.e., similar habitats that would be classified as presence) with the exception of
 575 heteroscedastic PNN, which rendered a multimodal mean partial dependence plot for the
 576 variable velocity (in black). However, in accordance with the maximum probabilistic values
 577 obtained for the SVM (Table 5), the partial dependence plots for this technique presented
 578 lower values for all plots (Fig. 9). Nevertheless, SVMs modify the classification threshold;
 579 thus, the microhabitats being considered suitable did not change substantially, which
 580 maintains the interpretation of these plots.

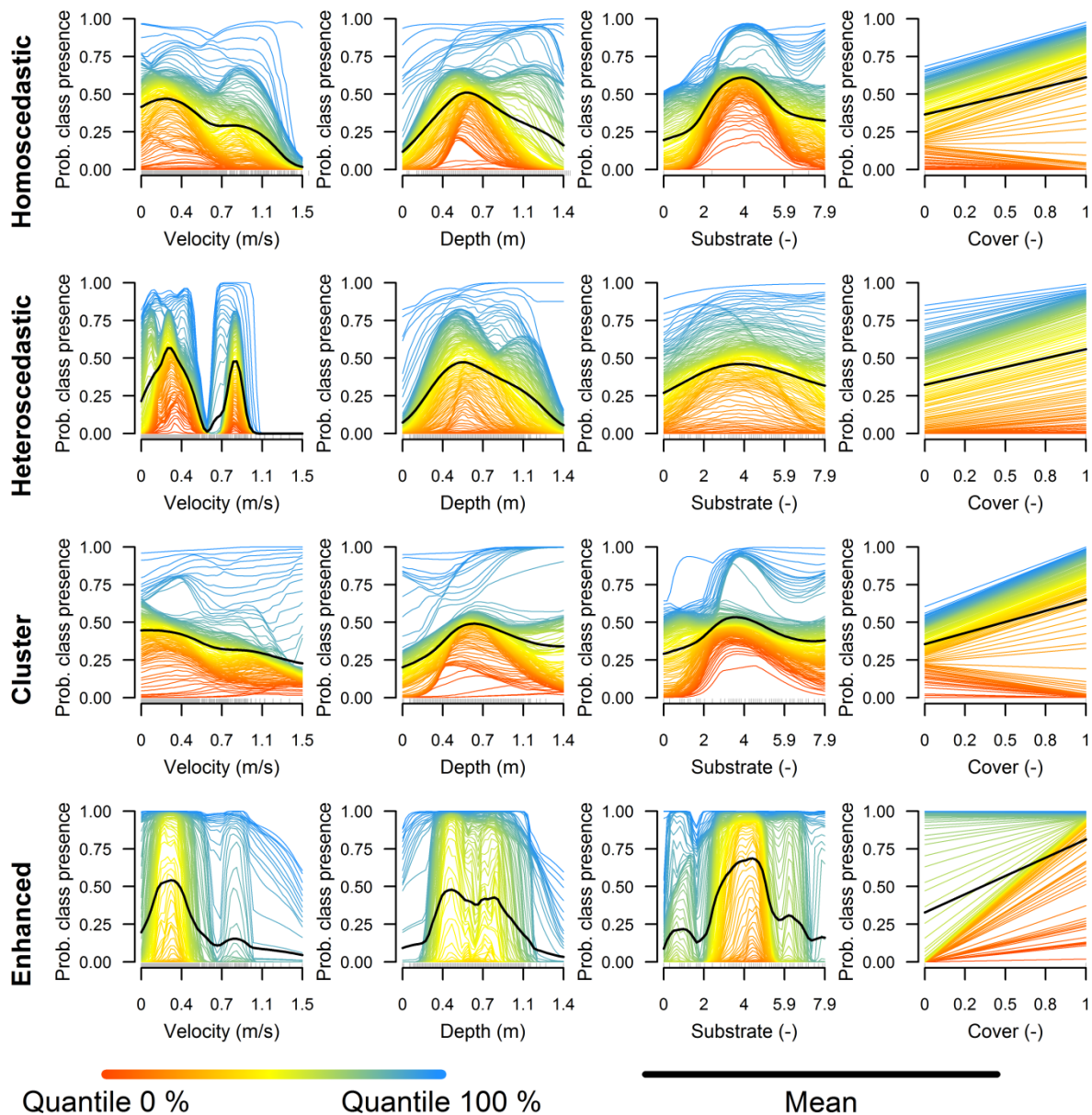
581 Setting apart the mean partial dependence plot (in black) for velocity obtained with the
 582 heteroscedastic PNN, Eastern Iberian chub presented the highest suitability in microhabitats
 583 with low flow velocity (approx. 0.3 m/s) and intermediate depth (approx. 0.6 m), and with
 584 mild coarseness – the optimal substrate index was approx. 4, which corresponds to fine
 585 gravel (64–256 mm) – and with cover present (i.e., cover = 1). Suitability decreased at the

586 extremes of the range of variables, with the exception of the cover variable. This decrease
587 was especially relevant for high velocity and low depth, and for fine substrate and no cover.
588 Nevertheless, the depicted quantiles revealed that the Eastern Iberian chub is a versatile
589 species that can select a microhabitat when some variables compensate for the low quality
590 of others. In accordance, mean unsuitable conditions at the extremes of the range of
591 variables (in black) presented high values of the probability of presence under particular
592 circumstances (coloured quantiles), which were caused by these infrequent occurrences of
593 the species. As a consequence, some microhabitats with high depth and coarse substrate
594 were evaluated positively, as well as some without cover, in the partial dependence plots of
595 the enhanced PNN.

596 According to the low $\sigma_{velocity}$, the heteroscedastic PNN exacerbated the mathematical effect
597 of the these infrequent occurrences; thus, the presence of four presence data within 0.730
598 and 0.856 m/s raised the probability of presence to the maximum. The opposite occurred
599 between 0.467 and 0.730 m/s, where the absence of presence patterns reduced the
600 probability of presence as far as zero. Enhanced PNN also presented relevant irregularities,
601 in spite of the reasonably smooth mean partial dependence plots (in black). It rendered
602 extreme values (i.e., zero and one) in almost every value of the evaluated range. From the
603 mathematical viewpoint, the occurrence of isolated presence data reduced the value of α_{mi}
604 for these patterns and consequently, the PNN rendered extreme values of the PDF when
605 approximating them. On the contrary, cluster PNN reduced such irregularities due to the
606 shrinkage in the number of training patterns, presenting smooth partial dependence plots.

607 Nevertheless their plots largely coincided with those for the homoscedastic PNN and SVM,
608 although SVM presented the smoothest plots of these three models (Fig. 9).

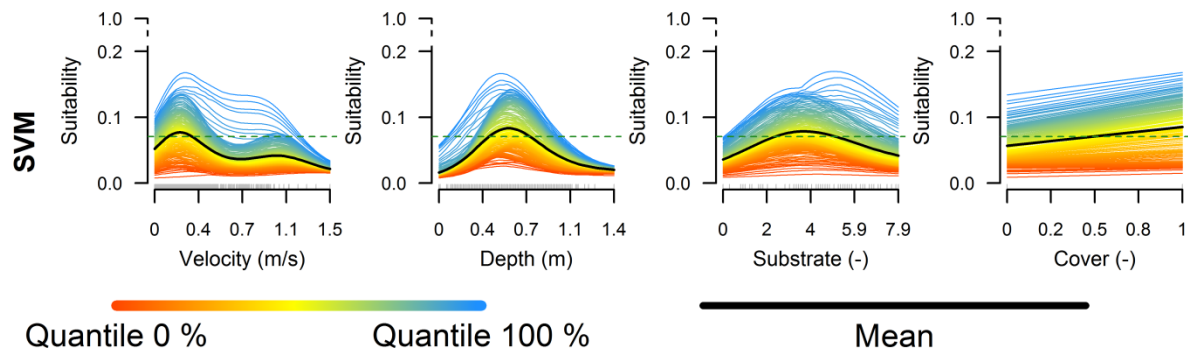
609



610

611 Fig. 8. Partial dependence plots, for the four approaches to develop probabilistic neural networks
612 (homoscedastic, heteroscedastic, cluster and enhanced), depicting the marginal relationship
613 between the suitability (i.e., probability of class presence) and the four microhabitat variables.
614

615



616

617 Fig. 9. Partial dependence plots, for the Support Vector Machine (SVM), depicting the marginal
618 relationship between the suitability (i.e., probability of class presence) and the four microhabitat
619 variables. The dashed line depicts the modified classification threshold.
620

621 4 Discussion

622 Four different approaches to develop PNNs have been successfully compared with SVMs
623 demonstrating that SVMs do not outperform every kind of PNN. Nonetheless, the SVM did
624 not present the best value in any of the calculated criteria. In addition, we obtained
625 relevant information about the microhabitat suitability for the Eastern Iberian chub.

626

627 4.1 Model characteristics

628 These four alternative PNNs span the two major contemporary approaches to improve
629 PNNs, which include the smoothing parameter optimisation and pattern neuron reduction
630 (Kusy and Zajdel, 2015; Ahmadlou and Adeli, 2010; Miguez et al., 2010; Li and Ma, 2008).

631

632 **4.1.1 Smoothing parameter optimisation**

633 Among the group of smoothing parameter optimisations, two of the most common
634 approaches have been tested, although other alternatives exist, such as different smoothing
635 parameters for each class (homoscedastic and heteroscedastic) (Zhong et al., 2007), which
636 can be extended to the extreme of one smoothing parameter per training pattern at the
637 expense of increasing the computational burden (Kusy and Zajdel, 2015). The former could
638 certainly be interesting, although it can be also tackled by employing prior probabilities or
639 uneven misclassification costs (discarded for this study) that may favour the desired class by
640 increasing the final value calculated for the corresponding PDF. In accordance, we
641 considered that the use of different smoothing parameters for each class may require a
642 dedicated study. Regarding the latter, from the ecological viewpoint heteroscedastic PNN
643 may potentially lead to unreliable models (Austin, 2007), although this approach rendered
644 one of the best performances. Therefore, we considered the optimisation of one smoothing
645 parameter per training pattern inappropriate because of the number of parameters and
646 thus increasing risk of overfitting. As a consequence, we would neither advocate
647 heteroscedasticity nor one smoothing parameter per training pattern without the adequate
648 scrutiny of the modelled habitat suitability.

649 This concern is also extendable for enhanced PNN, although it is indubitable that varying
650 the smoothing parameter to account for local densities and data inhomogeneity improves
651 model performance. Nonetheless, enhanced PNN achieved one of the highest mean values
652 of the fitness function by exclusively optimising two parameters. Enhanced PNNs modify
653 the value of the smoothing parameter based on the proportion of cases within the local

654 circle that are from the same class. However, the use of local circles to account for the data
655 inhomogeneity do not solve the impact caused by the presence of rare or infrequent data,
656 such as the presence data observed between 0.730 and 0.856 m/s, which appears isolated
657 in the input space (see violin plots in Fig. 7). Thus, even the result of a careful cross-
658 validation (e.g., repeated k-fold or leave-one-out) could be biased if the source data set is
659 insufficiently representative as a whole or if a relevant proportion of rare samples are
660 present (Grim and Hora, 2010), resulting in spiked PDFs, as observed in the corresponding
661 partial dependence plots.

662 With regard to the SVM, the γ parameter of the Gaussian kernel can be seen as the
663 smoothing parameters of the PNNs and, taking into account that they are constant across
664 the input space, the approach followed may resemble that described for the homoscedastic
665 version of the PNN. However, several variants of SVMs exist, which may render different
666 results. Although other authors disregarded this option (Wu et al., 2012), the most basic
667 one consists of varying the kernel function (R Muñoz-Mas et al., 2016d). Nevertheless, with
668 regard to the PNNs, different kernel density functions can also be selected to calculate the
669 PDFs (e.g., triangular, Epanechnikov or Gaussian). Consequently, the number of
670 combinations would be large; thus, we consider that such appealing comparison may also
671 require a dedicated study.

672 Interestingly, clustering has also been successfully applied as a pre-treatment for SVMs in
673 several ways. For instance, there are studies that tested the impact of different clustering
674 algorithms on accuracy and computational burden (e.g., Wang et al., 2007). Conversely,
675 although methodologically appealing, to the best of our knowledge SVMs did not present

any modelling approach analogous to the heteroscedastic and/or the enhanced variants of the PNNs where each axis or each pattern presents its own smoothing parameter σ . Thus, the equivalent to the enhanced approach for an SVM would be the local optimisation of a separate SVM for the neighbourhood of each training pattern. Although this strategy still needs to be the subject of dedicated research to be formally mathematised (e.g., the radii of the neighbourhood may also vary across the input space), it can be ventured that accounting for local densities or inhomogeneity in the training data should also lead to improved outcomes for SVMs. Consequently, we considered the ideas involving the enhanced variant and its stand-alone use, or in combination (e.g., cluster & enhanced PNNs), to be appealing.

On the other hand, the SVM rendered the most ecologically reliable partial dependence plots, although they could be considered deficient if outputs covering the entire feasible range are desired (R Muñoz-Mas et al., 2016a). For instance, SVM will render misleading results of the renowned Weighted Usable Area (WUA) (Bovee *et al.*, 1998). The WUA is calculated for a given flow as the product of the habitat area (e.g., pixels) and habitat suitability of the hydraulics of this area and summed across a river reach (R Muñoz-Mas et al., 2016a). However, given the mathematization of the WUA, a huge amount of low quality habitat may render similar total value as a small area of highly suitable habitat (Person *et al.*, 2014). This is not the case of the Suitable Area (SA), which is the sum of the areas where the models predicted presence (Person *et al.*, 2014). Therefore, the SVM proved only competent to calculate the SA (R Muñoz-Mas et al., 2016a). Previous experiences indicated data overlapping and prevalence as the main causes of this deficiency (R Muñoz-Mas et al.,

698 2016d, 2016a); thus, this study corroborated that Platt's approach for probability
699 calculation is unable to render proper probabilistic results for class-overlapped and low-
700 prevalence datasets (Platt, 2000). Nevertheless, this deficiency could be addressed by
701 employing clustering approaches to balance the data prevalence or alternative routines to
702 train SVMs that are particularly indicated to render reliable probabilistic outputs. Currently,
703 the most promising approach for the latter case is the routine implemented in the *R*
704 package *probsvm* (Zhang et al., 2013), which combines ideas from a number of sources
705 (Shin et al., 2014; Wang et al., 2008; Wu et al., 2004). However, it does not allow case
706 weighting. Consequently, in the end, it may require the use of resampling strategies or
707 balancing algorithms (e.g., SMOTE Chawla et al., 2002) that are unnecessary for PNNs.

708

709 **4.1.2 Pattern neuron reduction**

710 Clustering as a pre-treatment has been demonstrated to be proficient for the rapid training
711 of accurate PNNs. Nonetheless, taking into account the larger number of fitness function
712 evaluations performed, which was governed by the parameters *NP* and *steptol/reltol* (i.e.,
713 $10 \times \# \text{parameters}$ and $5 \times \# \text{parameters}$), the lapse of the optimisation for cluster PNN
714 should not be considered different than that for the SVM. However, other alternatives exist
715 (e.g., Kusy and Zajdel, 2015; Berthold and Diamond, 1998). Among the group of approaches
716 for pattern neuron reduction one popular approach with a number of examples (e.g.,
717 Narimani and Narimani, 2013) is the Dynamic Decay Adjustment (DDA) (Berthold and
718 Diamond, 1998). DDA adds sequentially each training pattern to the PNN, but exclusively
719 retains those patterns that are not redundant and/or in conflict with the remaining classes

720 (Berthold and Diamond, 1998). Based on the latter, DDA could be more accurate than our
721 cluster approach because it takes into account the distribution of every input class during
722 PNN growth. Nevertheless, it requires several epochs to converge, typically five (Berthold
723 and Diamond, 1998), which may lead to increasing computational costs. On the contrary,
724 compared to the remaining approaches, optimising a different number of cluster centres for
725 each class rendered high performance criteria; cluster PNN rendered the highest accuracy
726 (CCI) and Specificity (Sp). In addition, the partial dependence plots were ecologically reliable
727 because the clustering approach as a pre-treatment reduced the influence of rare data,
728 which typically compromises the reliability of the PNNs (Grim and Hora, 2010; Yang and
729 Chen, 1998). Furthermore, the approach followed to develop the cluster PNN could be
730 combined with heteroscedastic and/or enhanced PNNs (Chang et al., 2008; Yang and Chen,
731 1998). Therefore, we consider the combination of cluster PNN with other methods to be the
732 most promising approach for ecological studies. Accordingly, we expect these ideas to be
733 the subject of further research.

734

735 **4.2 Habitat suitability for the Eastern Iberian chub (*Squalius valentinus*)**

736 In spite of the ecologically unreliable partial dependence plots rendered by heteroscedastic
737 and enhanced PNNs, the five models largely converged on the optimal microhabitat for the
738 Eastern Iberian chub. Therefore, the species will preferentially occur in microhabitats with
739 low flow velocity – but not stagnated – of intermediate depth and substrate, and with cover
740 fundamentally present. This description broadly matches the general preferences of the
741 species suggested by Doadrio and Carmona (2006) who stated that the species prefers

742 moderate flowing reaches with clear water and gravel bottom, which in addition may fit the
743 habitat requirements of a number of Iberian species of the genus (e.g., Martelo et al., 2014;
744 Martínez-Capel et al., 2009; Santos and Ferreira, 2008). However, flexible microhabitat use
745 strategies are common among fishes inhabiting Mediterranean streams due to the long-
746 term adaptations to irregular flow regimes (Martelo et al., 2014). Thus, any comparison
747 with others species or studies should be made cautiously, as similarities may be due to
748 particularities, either spatial or temporal.

749 The optimal values for Eastern Iberian chub showed remarkable similitudes with those
750 obtained for *S. pyrenaicus*, perhaps the closest relative (Doadrio and Carmona, 2006), which
751 was studied in several river reaches of the central Iberian Peninsula (Martínez-Capel et al.,
752 2009). Thus, the only difference was the optimal value of depth for large individuals (> 10
753 cm), which tended to occupy deeper microhabitats (0.49 to 1.40 m) (Martínez-Capel et al.,
754 2009). Eastern Iberian chub also occurred in microhabitats similar to those occupied by *S.*
755 *torgalensis*, *S. carolitertii* and *S. aradensis*, all of which have been sampled in other
756 Mediterranean and temperate small streams of the Iberian Peninsula (Martelo et al., 2014;
757 Santos and Ferreira, 2008; Santos et al., 2004). This coincidence was especially relevant for
758 depth, substrate and, to a lesser extent, for cover – which was used less frequently by these
759 species – but the most remarkable difference occurred for velocity (Martelo et al., 2014;
760 Santos and Ferreira, 2008; Santos et al., 2004). However, this is most probably caused by
761 differences in the available microhabitats, which, in these studies, were dominated by
762 shallow and moderate-to-fast flowing riffles and runs (Martelo et al., 2014; Santos and
763 Ferreira, 2008). Taking into account that Eastern Iberian chub rarely exceed 20 cm (Alcaraz-

764 Hernández et al., 2015; Doadrio and Carmona, 2006) such a discrepancy can be caused by
765 the relatively small size of the species, which may lead to inferior natatorial capacity, as has
766 been demonstrated for other Iberian species (i.e., *S. carolitertii*) (Romão et al., 2012).
767 Nevertheless, while velocity may certainly be a limitation in the occurrence of Eastern
768 Iberian chub, we consider that depth is not. Nonetheless, in Vezza et al. (2015) different
769 results were obtained for what was originally classified as *S. pyrenaicus* based on the
770 morphologic characteristics of the specimens captured in the upper Cabriel that did not
771 match those described in Doadrio and Carmona (2006). However, in light of the information
772 contained in contemporary studies that performed genetic analyses (Perea, 2016 personal
773 communication; Perea and Doadrio, 2015), it is currently suspected that the *Squalius*
774 inhabiting the upper Cabriel is also *S. valentinus*. Therefore, following this supposition, in
775 Vezza et al. (2015) Eastern Iberian chub occurred principally in low gradient and depth
776 (from 1.25 up to 3.5 m) mesohabitats (i.e., pools) of intermediate granularity whereas the
777 presence of macrophytes (one of the considered cover types) presented an unequivocal
778 positive influence on the occurrence of chub. Therefore, we believe that, in further
779 microhabitat studies, Eastern Iberian chub will select deeper microhabitats if they present
780 some elements of cover. Such an asseveration will be supported by the aforementioned
781 ontogenetic shifts of habitat preferences towards deeper microhabitats (Martelo et al.,
782 2014; Martínez-Capel et al., 2009; Santos and Ferreira, 2008) and the generalised use of
783 cover elements observed in other species of the genus (Martelo et al., 2014; Pander and
784 Geist, 2010; Santos et al., 2004). Thereby, based on the experience gained in previous
785 studies, where the species is either certainly present (R Muñoz-Mas et al., 2016d; Costa et

786 al., 2012) or suspected to be present (Muñoz-Mas et al., 2017; Vezza et al., 2015), and
787 compared to other Mediterranean species of chub, such as the Peloponnesian *S. keadicus*
788 (Vardakas et al., 2017) or the native Iberian *S. pyrenaicus* (Martínez-Capel et al., 2009), we
789 consider that the Eastern Iberian chub is apparently one of the *Squalius* species least prone
790 to venture into mid-channel microhabitats. In accordance, despite the fact that distance to
791 shore was not measured, which is a common variable in studies performed at the
792 microhabitat scale (e.g., Vardakas et al., 2017; Martínez-Capel et al., 2009), we consider the
793 Eastern Iberian chub to be the *Squalius* species that is most likely to remain near banks the
794 majority of the time. Moreover, based on studies on other species of chub (Watkins et al.,
795 1997), this behaviour could in turn be caused either by the lack of cover typical of mid-
796 channel microhabitats or by the maximum body size achieved by the species, which is
797 inferior to that of other species. Nevertheless, these asseverations will require
798 confirmation, since there is evidence that, on the one hand, shoal and individual sizes
799 (Martelo et al., 2013) and, on the other hand, season (i.e., temperature and illumination),
800 affect *Squalius* activity (Santos and Ferreira, 2008; Baras and Nindaba, 1999).

801 Finally, although the species may be claimed to present a certain tendency towards
802 limnophilia, from the microscale point of view, our results corroborate the eurytopic nature
803 of what we suspect were Eastern Iberian chubs (Vezza et al., 2015). Consequently, although
804 the spread of the quantiles indicated the presence of remarkable interactions between the
805 four input variables, which could better be scrutinised with modelling approaches more
806 transparent, for instance, fuzzy logic or generalized additive models (see e.g., Muñoz-Mas et
807 al., 2016d, 2017), this study sheds novel insights on the habitat requirements of the species.

808 Therefore, we consider it will contribute to enhance environmental flow assessment and
809 the adequate implementation of management actions focused on habitat restoration and
810 species conservation (Martelo et al., 2013; Martínez-Capel et al., 2009; Santos et al., 2004).

811

812 **5 Conclusions**

813 This study compared four PNNs and a SVM for assessing habitat suitability of the Eastern
814 Iberian chub. Whereas heteroscedastic and enhanced PNNs achieved the highest accuracy,
815 these models exhibited ecologically unreliable partial dependence plots. In contrast,
816 homoscedastic and cluster PNNs rendered ecologically reliable partial dependence plots.

817 This could be explained by the inherent trade-off between model performance and
818 interpretability of partial dependence plots. Based on the results of cluster PNNs, we would
819 advocate combinations of approaches (e.g., cluster & heteroscedastic or cluster & enhanced
820 PNNs) to balance the accuracy-interpretability trade-off. From the partial dependence plots,
821 the Eastern Iberian chub proved to be a eurytopic species as it preferentially occurred, and
822 hence presented the largest probability of presence, in microhabitats with cover present,
823 low flow velocity (approx. 0.3 m/s) and intermediate depth (approx. 0.6 m) while the
824 optimal substrate corresponded to fine gravel (64–256 mm). This ecological information on
825 the Eastern Iberian chub should help the adequate implementation of management and
826 restoration actions for this vulnerable species. Although several aspects require further
827 research, we expect this study, and the annexed code, to promote the use of PNNs among

828 scientists in general, and among ecologists and conservationists in particular for species
829 distribution modelling and habitat suitability assessment.

830

831 **6 Acknowledgments**

832 The study has been partially funded by the national Research project IMPADAPT (CGL2013-
833 48424-C2-1-R) with MINECO (Spanish Ministry of Economy) and Feder funds and by the
834 Confederación Hidrográfica del Júcar (Spanish Ministry of Agriculture and Fisheries, Food
835 and Environment). This study was also supported in part by the University Research
836 Administration Center of the Tokyo University of Agriculture and Technology. Thanks to
837 María José Felipe for the review on the mathematical notation and to the two anonymous
838 reviewers who helped to improve the manuscript.

839

840 **7 References**

841 Abdollahnejad, A., Panagiotidis, D., Joybari, S.S., Surový, P., 2017. Prediction of dominant
842 forest tree species using quickbird and environmental data. *Forests* 8 (2).
843 10.3390/f8020042

844 Adeli, H., Panakkat, A., 2009. A probabilistic neural network for earthquake magnitude
845 prediction. *Neural Networks* 22 (7), 1018–1024. 10.1016/j.neunet.2009.05.003

846 Ahmadlou, M., Adeli, H., 2010. Enhanced probabilistic neural network with local decision
847 circles: A robust classifier. *Integr. Comput. Aided. Eng.* 17 (3), 197–210. 10.3233/ICA-

- 848 2010-0345
- 849 Alcaraz-Hernández, J.D., Martínez-Capel, F., Olaya-Marín, E.J., 2015. Length-weight
850 relationships of two endemic fish species in the Júcar River Basin, Iberian Peninsula. *J.*
851 *Appl. Ichthyol.* 31 (1), 246–247. 10.1111/jai.12625
- 852 Allouche, O., Tsoar, A., Kadmon, R., 2006. Assessing the accuracy of species distribution
853 models: prevalence, kappa and the true skill statistic (TSS). *J. Appl. Ecol.* 43 (6), 1223–
854 1232. 10.1111/j.1365-2664.2006.01214.x
- 855 Ardia, D., Boudt, K., Carl, P., Mullen, K.M., Peterson, B.G., 2011. Differential evolution with
856 deoptim. *R J.* 3 (1), 27–34.
- 857 Austin, M., 2007. Species distribution models and ecological theory: A critical assessment
858 and some possible new approaches. *Ecol. Modell.* 200 (1–2), 1–19.
859 10.1016/j.ecolmodel.2006.07.005
- 860 Baras, E., Nindaba, J., 1999. Seasonal and diel utilisation of inshore microhabitats by larvae
861 and juveniles of *Leuciscus cephalus* and *Leuciscus leuciscus*. *Environ. Biol. Fishes* 56 (1–
862 2), 183–197. 10.1023/A:1007594932734
- 863 Belousov, A.I., Verzakov, S.A., von Frese, J., 2002. A flexible classification approach with
864 optimal generalisation performance: support vector machines. *Chemom. Intell. Lab.*
865 *Syst.* 64 (1), 15–25. 10.1016/S0169-7439(02)00046-1
- 866 Ben-Hur, A., Weston, J., 2010. A User's Guide to Support Vector Machines, in: Carugo, O.,
867 Eisenhaber, F. (Eds.), *Data Mining Techniques for the Life Sciences*. Totowa, NJ, pp.
868 223–239.
- 869 Bennetsen, E., Gobeyn, S., Goethals, P.L.M., 2016. Species distribution models grounded in

- 870 ecological theory for decision support in river management. *Ecol. Modell.* 325, 1–12.
- 871 10.1016/j.ecolmodel.2015.12.016
- 872 Berrar, D.P., Downes, C.S., Dubitzky, W., 2003. Multiclass cancer classification using gene
873 expression profiling and probabilistic neural networks, in: Pacific Symposium on
874 Biocomputing. School of Biomedical Sciences, University of Ulster at Coleraine,
875 BT521SA, Northern Ireland., pp. 5–16.
- 876 Berthold, M.R., Diamond, J., 1998. Constructive training of probabilistic neural networks.
877 *Neurocomputing* 19 (1–3), 167–183. 10.1016/s0925-2312(97)00063-5
- 878 Bishop, C.M., 1995. Neural Networks for Pattern Recognition. New York, NY (USA).
- 879 Boavida, I., Dias, V., Ferreira, M.T., Santos, J.M., 2014. Univariate functions versus fuzzy
880 logic: Implications for fish habitat modeling. *Ecol. Eng.* 71, 533–538.
881 10.1016/j.ecoleng.2014.07.073
- 882 Bovee, K.D., 1986. Development and evaluation of habitat suitability criteria for use in the
883 instream flow incremental methodology, Instream Flow Information Paper 21. United
884 States Fish and Wildlife Service, Biological Report.
- 885 Bovee, K.D., Lamb, B.L., Bartholow, J.M., Stalnaker, C.B., Taylor, J., Henriksen, J., 1998.
886 Stream habitat analysis using the instream flow incremental methodology. Fort Collins,
887 CO (USA).
- 888 Breiman, L., Friedman, J.H., Olshen, R.A., Stone, C.J., Olshen, R.A., 1984. Classification and
889 Regression Trees, CRC Texts in Statistical Science. New York, NY (USA).
- 890 Burrascano, P., 1991. Learning vector quantization for the probabilistic neural network. IEEE
891 *Trans. neural networks* 2 (4), 458–461. 10.1109/72.88165

- 892 Casas-Mulet, R., King, E., Hoogeveen, D., Duong, L., Lakhanpal, G., Baldwin, T., et al., 2016.
- 893 Two decades of ecohydraulics: trends of an emerging interdiscipline. *J. Ecohydraulics*.
- 894 10.1080/24705357.2016.1251296
- 895 Chang, R.K.Y., Loo, C.K., Rao, M.V.C., 2009. Enhanced probabilistic neural network with data
- 896 imputation capabilities for machine-fault classification. *Neural Comput. Appl.* 18 (7),
- 897 791–800. 10.1007/s00521-008-0215-1
- 898 Chang, R.K.Y., Loo, C.K., Rao, M.V.C., 2008. A global k-means approach for autonomous
- 899 cluster initialization of probabilistic neural network. *Informatica* 32 (2), 219–225.
- 900 Chasset, P.O., 2013. PNN: Probabilistic neural network for the statistical language R.
- 901 Chawla, N. V., Bowyer, K.W., Hall, L.O., Kegelmeyer, W.P., 2002. SMOTE: Synthetic minority
- 902 over-sampling technique. *J. Artif. Intell. Res.* 16, 321–357. 10.1613/jair.953
- 903 Chen, G., Han, T.X., He, Z., Kays, R., Forrester, T., 2014. Deep convolutional neural network
- 904 based species recognition for wild animal monitoring, in: 2014 IEEE International
- 905 Conference on Image Processing, ICIP 2014. Paris (France), pp. 858–862.
- 906 Corne, S.A., Carver, S.J., Kunin, W.E., Lennon, J.J., van Hees, W.W.S., 2004. Predicting forest
- 907 attributes in southeast Alaska using artificial neural networks. *For. Sci.* 50 (2), 259–276.
- 908 Cornwell, W.K., Schwilk, D.W., Ackerly, D.D., 2006. A trait-based test for habitat filtering:
- 909 Convex hull volume. *Ecology* 87 (6), 1465–1471. 10.1890/0012-
- 910 9658(2006)87[1465:ATTFHF]2.0.CO;2
- 911 Costa, R.M.S., Martínez-Capel, F., Muñoz-Mas, R., Alcaraz-Hernández, J.D., Garofano-
- 912 Gómez, V., 2012. Habitat suitability modelling at mesohabitat scale and effects of dam
- 913 operation on the endangered Júcar nase, *Parachondrostoma arrigonis* (River Cabriel,

- 914 Spain). *River Res. Appl.* 28 (6), 740–752. 10.1002/rra.1598
- 915 Crisci, C., Ghattas, B., Perera, G., 2012. A review of supervised machine learning algorithms
916 and their applications to ecological data. *Ecol. Modell.* 240 (0), 113–122.
917 10.1016/j.ecolmodel.2012.03.001
- 918 Dimitriadou, E., Hornik, K., Leisch, F., Meyer, D., Weingessel, D., 2011. e1071: Misc
919 Functions of the Department of Statistics, Probability Theory Group (Formerly: e1071),
920 TU Wien (Austria).
- 921 Doadrio, I., Carmona, J.A., 2006. Phylogenetic overview of the genus *Squalius*
922 (Actinopterygii, Cyprinidae) in the Iberian Peninsula, with description of two new
923 species. *Cybium* 30 (3), 199–214.
- 924 Eberenz, J., Verbesselt, J., Herold, M., Tsendlbazar, N.-E., Sabatino, G., Rivolta, G., 2016.
925 Evaluating the potential of proba-v satellite image time series for improving lc
926 classification in semi-arid african landscapes. *Remote Sens.* 8 (12). 10.3390/rs8120987
- 927 Elith, J., Graham, C.H., 2009. Do they? How do they? Why do they differ? on finding reasons
928 for differing performances of species distribution models. *Ecography (Cop.)*. 32 (1), 66–
929 77. 10.1111/j.1600-0587.2008.05505.x
- 930 Ellis, E.C., Klein Goldewijk, K., Siebert, S., Lightman, D., Ramankutty, N., 2010.
931 Anthropogenic transformation of the biomes, 1700 to 2000. *Glob. Ecol. Biogeogr.* 19
932 (5), 589–606. 10.1111/j.1466-8238.2010.00540.x
- 933 Evans, J.S., Murphy, M.A., Holden, Z.A., Cushman, S.A., 2011. Modeling species distribution
934 and change using Random Forests, in: Drew, C.A., Wiersma, Y.F., Huettmann, F. (Eds.),
935 Predictive Species and Habitat Modeling in Landscape Ecology. New York, NY, pp. 139–

- 936 159.
- 937 Evans, M.E.K., Merow, C., Record, S., McMahon, S.M., Enquist, B.J., 2016. Towards Process-
938 based Range Modeling of Many Species. Trends Ecol. Evol. 31 (11).
939 10.1016/j.tree.2016.08.005
- 940 Friedman, J.H., 2001. Greedy function approximation: A gradient boosting machine. Ann.
941 Stat. 29 (5), 1189–1232. 10.1214/aos/1013203451
- 942 Fukuda, S., De Baets, B., 2016. Data prevalence matters when assessing species' responses
943 using data-driven species distribution models. Ecol. Inform. 32, 69–78.
944 10.1016/j.ecoinf.2016.01.005
- 945 Fukuda, S., De Baets, B., Waegeman, W., Verwaeren, J., Mouton, A.M., 2013. Habitat
946 prediction and knowledge extraction for spawning European grayling (*Thymallus*
947 *thymallus* L.) using a broad range of species distribution models. Environ. Model. Softw.
948 47, 1–6. 10.1016/j.envsoft.2013.04.005
- 949 Fukuda, S., Tanakura, T., Hiramatsu, K., Harada, M., 2014. Assessment of spatial habitat
950 heterogeneity by coupling data-driven habitat suitability models with a 2D
951 hydrodynamic model in small-scale streams. Ecol. Inform. 10.1016/j.ecoinf.2014.10.003
- 952 Gibbs, M.S., Dandy, G.C., Maier, H.R., 2008. A genetic algorithm calibration method based
953 on convergence due to genetic drift. Inf. Sci. (Ny). 178 (14), 2857–2869.
954 10.1016/j.ins.2008.03.012
- 955 Grim, J., Hora, J., 2010. Computational properties of probabilistic neural networks, in:
956 Diamantaras, K., Duch, W., Iliadis, L.S. (Eds.), 20th International Conference on Artificial
957 Neural Networks. Thessaloniki (Greece), pp. 31–40.

- 958 Guisan, A., Tingley, R., Baumgartner, J.B., Naujokaitis-Lewis, I., Sutcliffe, P.R., Tulloch, A.I.T.,
959 et al., 2013. Predicting species distributions for conservation decisions. *Ecol. Lett.* 16
960 (12), 1424–1435. 10.1111/ele.12189
- 961 Gumbel, E.J., 1939. La probabilité des hypothèses. *Comptes Rendus l'Académie des Sci.* 209,
962 645–647.
- 963 Gutierrez, P.A., Perez-Ortiz, M., Sanchez-Monedero, J., Fernandez-Navarro, F., Hervas-
964 Martinez, C., 2016. Ordinal Regression Methods: Survey and Experimental Study. *IEEE
965 Trans. Knowl. Data Eng.* 28 (1), 127–146. 10.1109/TKDE.2015.2457911
- 966 Habersack, H., Haspel, D., Kondolf, M., 2014. Large Rivers in the Anthropocene: Insights and
967 tools for understanding climatic, land use, and reservoir influences. *Water Resour. Res.*
968 50 (5), 3641–3646. 10.1002/2013WR014731
- 969 Hajmeer, M., Basheer, I., 2002. A probabilistic neural network approach for modeling and
970 classification of bacterial growth/no-growth data. *J. Microbiol. Methods* 51 (2), 217–
971 226. 10.1016/S0167-7012(02)00080-5
- 972 Hastie, T.J., Tibshirani, R.J., 1990. Generalized Additive Models, Monographs on Statistics &
973 Applied Probability. London, (UK).
- 974 Howley, T., Madden, M.G., 2005. The genetic kernel support vector machine: Description
975 and evaluation. *Artif. Intell. Rev.* 24 (3–4), 379–395. 10.1007/s10462-005-9009-3
- 976 Huang, C.-L., Wang, C.-J., 2006. A GA-based feature selection and parameters optimization
977 for support vector machines. *Expert Syst. Appl.* 31 (2), 231–240.
978 10.1016/j.eswa.2005.09.024
- 979 Hutchinson, G.E., 1957. Population studies – animal ecology and demography – concluding

- 980 remarks, in: Cold Spring Harbor Symposia on Quantitative Biology. pp. 415–427.
- 981 IUCN, 2016. The IUCN Red List of Threatened Species.
- 982 Jain, A.K., 2010. Data clustering: 50 years beyond K-means. Pattern Recognit. Lett. 31 (8),
983 651–666. 10.1016/j.patrec.2009.09.011
- 984 Jin, X., Cheu, R.L., Srinivasan, D., 2002. Development and adaptation of constructive
985 probabilistic neural network in freeway incident detection. Transp. Res. Part C Emerg.
986 Technol. 10 (2), 121–147. 10.1016/S0968-090X(01)00007-9
- 987 Jowett, I.G., Davey, A.J.H., 2007. A comparison of composite habitat suitability indices and
988 generalized additive models of invertebrate abundance and fish presence-habitat
989 availability. Trans. Am. Fish. Soc. 136 (2), 428–444. 10.1577/t06-104.1
- 990 Kaufman, L., Rousseeuw, P.J., 1987. Clustering by means of medoids, in: Dodge, Y. (Ed.),
991 Statistical Data Analysis Based on the L1 Norm and Related Methods. Amsterdam
992 (Netherlands), pp. 405–416.
- 993 Kohonen, T., 1982. Self-organized formation of topologically correct feature maps. Biol.
994 Cybern. 43 (1), 59–69. 10.1007/BF00337288
- 995 Kusy, M.I., Zajdel, R., 2015. Application of Reinforcement Learning Algorithms for the
996 Adaptive Computation of the Smoothing Parameter for Probabilistic Neural Network.
997 IEEE Trans. Neural Networks Learn. Syst. 26 (9), 2163–2175.
998 10.1109/TNNLS.2014.2376703
- 999 LaDeau, S.L., Han, B.A., Rosi-Marshall, E.J., Weathers, K.C., 2016. The Next Decade of Big
1000 Data in Ecosystem Science. Ecosystems 1–10. 10.1007/s10021-016-0075-y
- 1001 Li, L., Ma, G., 2008. Optimizing the Performance of Probabilistic Neural Networks Using PSO

- 1002 in the Task of Traffic Sign Recognition, in: Advanced Intelligent Computing Theories and
1003 Applications. With Aspects of Artificial Intelligence. Berlin/Heidelberg (Germany), pp.
1004 90–98.
- 1005 Liaw, A., Wiener, M., 2002. Classification and regression by randomForest. R News 3 (2), 18–
1006 22.
- 1007 Lorenz, A.W., Stoll, S., Sundermann, A., Haase, P., 2013. Do adult and YOY fish benefit from
1008 river restoration measures? Ecol. Eng. 61, Part A (0), 174–181.
1009 10.1016/j.ecoleng.2013.09.027
- 1010 Maceda-Veiga, A., 2013. Towards the conservation of freshwater fish: Iberian Rivers as an
1011 example of threats and management practices. Rev. Fish Biol. Fish. 23 (1), 1–22.
1012 10.1007/s11160-012-9275-5
- 1013 Maechler, M., Rousseeuw, P., Struyf, A., Hubert, M., Hornik, K., 2016. cluster: Cluster
1014 Analysis Basics and Extensions.
- 1015 Martelo, J., Grossman, G.D., Filomena Magalhães, M., 2013. Extrinsic and intrinsic factors
1016 influence daily activity of a Mediterranean cyprinid. Ecol. Freshw. Fish 22 (2), 307–316.
1017 10.1111/eff.12027
- 1018 Martelo, J., Grossman, G.D., Porto, M., Filomena Magalhães, M., 2014. Habitat patchiness
1019 affects distribution and microhabitat use of endangered Mira chub *Squalius torgalensis*
1020 (Actinopterygii, Cypriniformes). Hydrobiologia 732 (1), 93–109. 10.1007/s10750-014-
1021 1850-4
- 1022 Martínez-Capel, F., García De Jalón, D., Werenitzky, D., Baeza, D., Rodilla-Alamá, M., 2009.
1023 Microhabitat use by three endemic Iberian cyprinids in Mediterranean rivers (Tagus

- 1024 River Basin, Spain). *Fish. Manag. Ecol.* 16 (1), 52–60. 10.1111/j.1365-2400.2008.00645.x
- 1025 McCulloch, W.S., Pitts, W., 1943. A logical calculus of the ideas immanent in nervous
1026 activity. *Bull. Math. Biophys.* 5 (4), 115–133. 10.1007/BF02478259
- 1027 Miguez, R., Georgopoulos, M., Kaylani, A., 2010. G-PNN: A genetically engineered
1028 probabilistic neural network. *Nonlinear Anal.* 73 (6), 1783–1791.
1029 10.1016/j.na.2010.04.080
- 1030 Modaresi, F., Araghinejad, S., 2014. A comparative assessment of support vector machines,
1031 probabilistic neural networks, and K-nearest neighbor algorithms for water quality
1032 classification. *Water Resour. Manag.* 28 (12), 4095–4111. 10.1007/s11269-014-0730-z
- 1033 Moguerza, J.M., Muñoz, A., 2006. Support vector machines with applications. *Stat. Sci.* 21
1034 (3), 322–336. 10.1214/088342306000000493
- 1035 Mouton, A.M., Alcaraz-Hernández, J.D., De Baets, B., Goethals, P.L.M., Martínez-Capel, F.,
1036 2011. Data-driven fuzzy habitat suitability models for brown trout in Spanish
1037 Mediterranean rivers. *Environ. Model. Softw.* 26 (5), 615–622.
1038 10.1016/j.envsoft.2010.12.001
- 1039 Mouton, A.M., De Baets, B., Goethals, P.L.M., 2010. Ecological relevance of performance
1040 criteria for species distribution models. *Ecol. Modell.* 221 (16), 1995–2002.
1041 10.1016/j.ecolmodel.2010.04.017
- 1042 Mouton, A.M., Jowett, I., Goethals, P.L.M., De Baets, B., 2009. Prevalence-adjusted
1043 optimisation of fuzzy habitat suitability models for aquatic invertebrate and fish species
1044 in New Zealand. *Ecol. Inform.* 4 (4), 215–225. 10.1016/j.ecoinf.2009.07.006
- 1045 Mullen, K.M., Ardia, D., Gil, D.L., Windover, D., Cline, J., 2011. DEoptim: An R package for

1046 global optimization by differential evolution. *J. Stat. Softw.* 40 (6), 1–26.
1047 10.18637/jss.v040.i06

1048 Muniz, A.M.S., Liu, H., Lyons, K.E., Pahwa, R., Liu, W., Nobre, F.F., et al., 2010. Comparison
1049 among probabilistic neural network, support vector machine and logistic regression for
1050 evaluating the effect of subthalamic stimulation in Parkinson disease on ground
1051 reaction force during gait. *J. Biomech.* 43 (4), 720–6. 10.1016/j.biomech.2009.10.018

1052 Muñoz-Mas, R., Costa, R.M.S., Martínez-Capel, F., Alcaraz-Hernández, J.D., 2017.
1053 Microhabitat competition between Iberian fish species and the endangered Júcar nase
1054 (*Parachondrostoma arrigonis*; Steindachner, 1866). *J. Ecohydraulics* 0 (0), 1–23.
1055 10.1080/24705357.2016.1276417

1056 Muñoz-Mas, R., Fukuda, S., Vezza, P., Martínez-Capel, F., 2016. Comparing four methods for
1057 decision-tree induction: A case study on the invasive Iberian gudgeon (*Gobio lozanoi*;
1058 *Doadrio and Madeira*, 2004). *Ecol. Inform.* 34, 22–34. 10.1016/j.ecoinf.2016.04.011

1059 Muñoz-Mas, R., Lopez-Nicolas, A., Martínez-Capel, F., Pulido-Velazquez, M., 2016a. Shifts in
1060 the suitable habitat available for brown trout (*Salmo trutta* L.) under short-term
1061 climate change scenarios. *Sci. Total Environ.* 544, 686–700.
1062 10.1016/j.scitotenv.2015.11.147

1063 Muñoz-Mas, R., Martínez-Capel, F., Alcaraz-Hernández, J.D., Mouton, A.M., 2016b. On
1064 species distribution modelling, spatial scales and environmental flow assessment with
1065 Multi-Layer Perceptron Ensembles: A case study on the redfin barbel (*Barbus haasi*;
1066 *Mertens*, 1925). *Limnol. - Ecol. Manag. Inl. Waters.* 10.1016/j.limno.2016.09.004

1067 Muñoz-Mas, R., Martínez-Capel, F., Garófano-Gómez, V., Mouton, A.M., 2014. Application

1068 of probabilistic neural networks to microhabitat suitability modelling for adult brown
1069 trout (*Salmo trutta* L.) in Iberian rivers. Environ. Model. Softw. 59 (0), 30–43.
1070 10.1016/j.envsoft.2014.05.003

1071 Muñoz-Mas, R., Martínez-Capel, F., Schneider, M., Mouton, A.M., 2012. Assessment of
1072 brown trout habitat suitability in the Jucar River Basin (Spain): Comparison of data-
1073 driven approaches with fuzzy-logic models and univariate suitability curves. Sci. Total
1074 Environ. 440, 123–131. 10.1016/j.scitotenv.2012.07.074

1075 Muñoz-Mas, R., Papadaki, C., Martínez-Capel, F., Zogaris, S., Ntoanidis, L., Dimitriou, E.,
1076 2016c. Generalized additive and fuzzy models in environmental flow assessment: A
1077 comparison employing the West Balkan trout (*Salmo fariooides*; Karaman, 1938). Ecol.
1078 Eng. 91, 365–377. 10.1016/j.ecoleng.2016.03.009

1079 Muñoz-Mas, R., Vezza, P., Alcaraz-Hernández, J.D., Martínez-Capel, F., 2016d. Risk of
1080 invasion predicted with support vector machines: a case study on northern pike (*Esox*
1081 *Lucius*, L.) and bleak (*Alburnus alburnus*, L.). Ecol. Modell. 342, 123–134.
1082 10.1016/j.ecolmodel.2016.10.006

1083 Narimani, R., Narimani, A., 2013. Classification credit dataset using particle swarm
1084 optimization and probabilistic neural network models based on the dynamic decay
1085 learning algorithm. Autom. Control Intell. Syst. 1 (5), 103–112.
1086 10.11648/j.acis.20130105.12

1087 Öğüt, H., Aktaş, R., Alp, A., Doğanay, M.M., 2009. Prediction of financial information
1088 manipulation by using support vector machine and probabilistic neural network. Expert
1089 Syst. Appl. 36 (3), 5419–5423. 10.1016/j.eswa.2008.06.055

- 1090 Olden, J.D., Lawler, J.J., Poff, N.L., 2008. Machine learning methods without tears: a primer
1091 for ecologists. *Q. Rev. Biol.* 83 (2), 171–193. 10.1086/587826
- 1092 Oliva, D., Cuevas, E., 2017. An introduction to machine learning, in: *Advances and*
1093 *Applications of Optimised Algorithms in Image Processing. Intelligent Systems*
1094 *Reference Library*, Vol 117. Cham (Switzerland), pp. 1–11.
- 1095 Osuna, E., Freund, R., Girosi, F., 1997. Training support vector machines: An application to
1096 face detection, in: Anonimous (Ed.), *Proceedings of the 1997 IEEE Computer Society*
1097 *Conference on Computer Vision and Pattern Recognition*. Cambridge, MA (USA), pp.
1098 130–136.
- 1099 Pander, J., Geist, J., 2010. Seasonal and spatial bank habitat use by fish in highly altered
1100 rivers - a comparison of four different restoration measures. *Ecol. Freshw. Fish* 19 (1),
1101 127–138. 10.1111/j.1600-0633.2009.00397.x
- 1102 Parzen, E., 1962. On Estimation of a Probability Density Function and Mode. *Ann. Math.*
1103 *Stat.* 33 (3), 13–1065.
- 1104 Perea, S., Doadrio, I., 2015. Phylogeography, historical demography and habitat suitability
1105 modelling of freshwater fishes inhabiting seasonally fluctuating mediterranean river
1106 systems: A case study using the iberian cyprinid *Squalius valentinus*. *Mol. Ecol.* 24 (14).
1107 10.1111/mec.13274
- 1108 Person, E., Bieri, M., Peter, A., Schleiss, A.J., 2014. Mitigation measures for fish habitat
1109 improvement in Alpine rivers affected by hydropower operations. *Ecohydrology* 7 (2),
1110 580–599. <http://dx.doi.org/10.1002/eco.1380>
- 1111 Platt, J., 2000. Probabilistic outputs for support vector machines and comparisons to

1112 regularized likelihood methods, in: Smola, A.J., Bartlett, P.J. (Eds.), *Advances in Large*
1113 *Margin Classifiers*. Cambridge, MA (USA), pp. 61–74.

1114 Platts, P.J., McClean, C.J., Lovett, J.C., Marchant, R., 2008. Predicting tree distributions in an
1115 East African biodiversity hotspot: model selection, data bias and envelope uncertainty.
1116 *Ecol. Modell.* 218 (1–2), 121–134. 10.1016/j.ecolmodel.2008.06.028

1117 Poff, N.L., Richter, B.D., Arthington, A.H., Bunn, S.E., Naiman, R.J., Kendy, E., et al., 2010. The
1118 ecological limits of hydrologic alteration (ELOHA): a new framework for developing
1119 regional environmental flow standards. *Freshw. Biol.* 55 (1), 147–170. 10.1111/j.1365-
1120 2427.2009.02204.x

1121 Quinlan, J.R., 1992. Learning with continuous classes, in: The 5th Australian Joint
1122 Conference on AI. Sydney (Australia), pp. 343–348.

1123 R Core Team, 2015. R: A language and environment for statistical computing.

1124 Raleigh, R.F., Zuckerman, L.D., Nelson, P.C., 1986. Habitat suitability index models and
1125 instream flow suitability curves: brown trout, revised. Washington DC, (USA).

1126 Reineking, B., Schröder, B., 2006. Constrain to perform: Regularization of habitat models.
1127 *Ecol. Modell.* 193 (3–4), 675–690. 10.1016/j.ecolmodel.2005.10.003

1128 Romão, F., Quintella, B.R., Pereira, T.J., Almeida, P.R., 2012. Swimming performance of two
1129 Iberian cyprinids: The Tagus nase *Pseudochondrostoma polylepis* (Steindachner, 1864)
1130 and the bordallo *Squalius carolitertii* (Doadrio, 1988). *J. Appl. Ichthyol.* 28 (1), 26–30.
1131 10.1111/j.1439-0426.2011.01882.x

1132 Rosenblatt, M., 1956. Remarks on Some Nonparametric Estimates of a Density Function.
1133 *Ann. Math. Stat.* 27 (3), 832–837. 10.1214/aoms/1177728190

- 1134 Rüger, N., Schlüter, M., Matthies, M., 2005. A fuzzy habitat suitability index for *Populus*
1135 *euphratica* in the Northern Amudarya delta (Uzbekistan). *Ecol. Modell.* 184 (2–4), 313–
1136 328. 10.1016/j.ecolmodel.2004.10.010
- 1137 Santos, J.M., Ferreira, M.T., 2008. Microhabitat use by endangered Iberian cyprinids nase
1138 *Iberochondrostoma almacai* and chub *Squalius aradensis*. *Aquat. Sci.* 70 (3), 272–281.
1139 10.1007/s00027-008-8037-x
- 1140 Santos, J.M., Godinho, F.N., Ferreira, M.T., 2004. Microhabitat use by Iberian nase
1141 *Chondrostoma polylepis* and Iberian chub *Squalius carolitertii* in three small streams,
1142 north-west Portugal. *Ecol. Freshw. Fish* 13 (3), 223–230. 10.1111/j.1600-
1143 0633.2004.00054.x
- 1144 Schmidhuber, J., 2015. Deep learning in neural networks: An overview. *Neural Networks* 61,
1145 85–117. 10.1016/j.neunet.2014.09.003
- 1146 Shin, S.J., Wu, Y., Zhang, H.H., 2014. Two-Dimensional Solution Surface for Weighted
1147 Support Vector Machines. *J. Comput. Graph. Stat.* 23 (2), 383–402.
1148 10.1080/10618600.2012.761139
- 1149 Shiroyama, R., Yoshimura, C., 2016. Assessing bluegill (*Lepomis macrochirus*) habitat
1150 suitability using partial dependence function combined with classification approaches.
1151 *Ecol. Inform.* 35, 9–18. 10.1016/j.ecoinf.2016.06.005
- 1152 Siira, A., Erkinaro, J., Jounela, P., Suuronen, P., 2009. Run timing and migration routes of
1153 returning Atlantic salmon in the Northern Baltic Sea: implications for fisheries
1154 management. *Fish. Manag. Ecol.* 16 (3), 177–190. 10.1111/j.1365-2400.2009.00654.x
- 1155 Sousa, R., Yevseyeva, I., da Costa, J.F.P., Cardoso, J.S., 2013. Multicriteria Models for

- 1156 Learning Ordinal Data: A Literature Review, in: Yang, X.-S. (Ed.), Artificial Intelligence,
1157 Evolutionary Computing and Metaheuristics. Berlin/Heidelberg (Germany), pp. 109–
1158 138.
- 1159 Specht, D.F., 1992. Enhancements to probabilistic neural networks, in: [Proceedings 1992]
1160 IJCNN International Joint Conference on Neural Networks. pp. 761–768.
- 1161 Specht, D.F., 1990. Probabilistic neural networks. *Neural Networks* 3 (1), 109–118.
1162 10.1016/0893-6080(90)90049-Q
- 1163 Specht, D.F., 1989. Probabilistic neural networks (a one-pass learning method) and potential
1164 applications, in: Western Electronic Show and Convention (WESCON). San Francisco, CA
1165 (USA), pp. 780–785.
- 1166 Specht, D.F., Romsdahl, H., 1994. Experience with adaptive probabilistic neural networks
1167 and adaptive general regression neural networks, in: Proceedings of 1994 IEEE
1168 International Conference on Neural Networks (ICNN'94). Orlando, FL (USA), pp. 1203–
1169 1208.
- 1170 Stein, G., Chen, B., Wu, A.S., Hua, K.A., 2005. Decision tree classifier for network intrusion
1171 detection with GA-based feature selection, in: Proceedings of the 43rd Annual
1172 Southeast Regional Conference on - ACM-SE 43. New York, NY (USA), p. 136.
- 1173 Storn, R., Price, K., 1997. Differential Evolution – A Simple and Efficient Heuristic for global
1174 Optimization over Continuous Spaces. *J. Glob. Optim.* 11 (4), 341–359.
1175 10.1023/A:1008202821328
- 1176 Tharme, R.E., 2003. A global perspective on environmental flow assessment: Emerging
1177 trends in the development and application of environmental flow methodologies for

- 1178 rivers. *River Res. Appl.* 19 (5–6), 397–441. 10.1002/rra.736
- 1179 Tierno de Figueroa, J.M., López-Rodríguez, M.J., Fenoglio, S., Sánchez-Castillo, P., Fochetti,
1180 R., 2013. Freshwater biodiversity in the rivers of the Mediterranean Basin.
1181 *Hydrobiologia* 719 (1), 137–186. 10.1007/s10750-012-1281-z
- 1182 Tricarico, E., 2012. A review on pathways and drivers of use regarding non-native
1183 freshwater fish introductions in the Mediterranean region. *Fish. Manag. Ecol.* 19 (2),
1184 133–141. 10.1111/j.1365-2400.2011.00834.x
- 1185 Van Der Maaten, L., Hinton, G., 2008. Visualizing data using t-SNE. *J. Mach. Learn. Res.* 9.
- 1186 Vapnik, V., 1995. The nature of statistical learning theory, Information Science and
1187 Statistics. New York, NY (USA).
- 1188 Vardakas, L., Kalogianni, E., Papadaki, C., Vavalidis, T., Mentzafou, A., Koutsoubas, D., et al.,
1189 2017. Defining critical habitat conditions for the conservation of three endemic and
1190 endangered cyprinids in a Mediterranean intermittent river before the onset of
1191 drought. *Aquat. Conserv. Mar. Freshw. Ecosyst.* na (na), 1–11. 10.1002/aqc.2735
- 1192 Verma, H.K., 2008. Radial basis probabilistic neural network for differential protection of
1193 power transformer. *IET Gener. Transm. Distrib.* 2 (1), 43–52(9). 10.1049/iet-gtd:
1194 20070037
- 1195 Vezza, P., Muñoz-Mas, R., Martínez-Capel, F., Mouton, A., 2015. Random forests to evaluate
1196 biotic interactions in fish distribution models. *Environ. Model. Softw.* 67, 173–183.
1197 10.1016/j.envsoft.2015.01.005
- 1198 Wang, J., Neskovic, P., Cooper, L.N., 2007. Selecting Data for Fast Support Vector Machines
1199 Training, in: Kacprzyk, J. (Ed.), Trends in Neural Computation. Berlin/Heidelberg

- 1200 (Germany), pp. 61–84.
- 1201 Wang, J., Shen, X., Liu, Y., 2008. Probability Estimation for Large-Margin Classifiers.
- 1202 Biometrika 95 (1), 149–167.
- 1203 Watkins, M.S., Doherty, S., Copp, G.H., 1997. Microhabitat use by 0+ and older fishes in a
- 1204 small English chalk stream. *J. Fish Biol.* 50 (5), 1010–1024. 10.1006/jfbi.1996.0363
- 1205 Werbos, P.J., 1982. Applications of advances in nonlinear sensitivity analysis, in: System
- 1206 Modeling and Optimization. Berlin/Heidelberg (Germany), pp. 762–770.
- 1207 Wisz, M.S., Hijmans, R.J., Li, J., Peterson, A.T., Graham, C.H., Guisan, A., et al., 2008. Effects
- 1208 of sample size on the performance of species distribution models. *Divers. Distrib.* 14
- 1209 (5), 763–773. 10.1111/j.1472-4642.2008.00482.x
- 1210 Wu, T.-F., Lin, C.-J., Weng, R.C., 2004. Probability estimates for multi-class classification by
- 1211 pairwise coupling. *J. Mach. Learn. Res.* 5, 975–1005.
- 1212 Wu, W.-J., Lin, S.-W., Moon, W.K., 2012. Combining support vector machine with genetic
- 1213 algorithm to classify ultrasound breast tumor images. *Comput. Med. Imaging Graph.* 36
- 1214 (8), 627–633. 10.1016/j.compmedimag.2012.07.004
- 1215 Yang, Z.R., Chen, S., 1998. Robust maximum likelihood training of heteroscedastic
- 1216 probabilistic neural networks. *Neural Networks* 11 (4), 739–747. 10.1016/S0893-
- 1217 6080(98)00024-0
- 1218 Yano, K., 2016. AI for taking on the challenges of an unpredictable era. *Hitachi Rev.* 65 (6),
- 1219 92–112.
- 1220 Zhang, C., Shin, S.J., Wang, J., Wu, Y., Zhang, H.H., Liu, Y., 2013. probsvm: Class probability
- 1221 estimation for Support Vector Machines.

1222 Zhong, M., Coggeshall, D., Ghaneie, E., Pope, T., Rivera, M., Georgopoulos, M., et al., 2007.

1223 Gap-based estimation: Choosing the smoothing parameters for probabilistic and

1224 general regression neural networks. *Neural Comput.* 19 (10), 2840–2864.

1225 10.1162/neco.2007.19.10.2840

1226 Zurell, D., Elith, J., Schröder, B., 2012. Predicting to new environments: tools for visualizing

1227 model behaviour and impacts on mapped distributions. *Divers. Distrib.* 18 (6), 628–634.

1228 10.1111/j.1472-4642.2012.00887.x

1229